Suppression of ANXA4 expression improves platinum sensitivity *in vivo*

To determine whether ANXA4 knockdown in clear cell carcinoma cells improved platinum sensitivity *in vivo*, NC7 and Y4 cells were subcutaneously injected in ICR *nu/nu* mice. One week after inoculation with the tumour cells, the mice were randomised into 2 groups and received cisplatin or PBS *i.p.* twice a week for 4 weeks. The tumour growth rate in the absence of drugs was similar for both cell lines (Figs. 2A and 2B). Cisplatin treatment had very little effect on NC7 cells (Fig. 2A), but tumour volume markedly decreased in Y4 cells (Fig. 2B). Cisplatin treatment significantly decreased tumour growth in Y4 cells (87.4 ± 1.8%) compared with NC7 cells (-1.1 ± 18.0%; $p < 0.01$; Fig. 2C). These results showed that ANXA4 knockdown in the RMG-I cell line significantly attenuated resistance to cisplatin *in vivo*.

The annexin repeat domain is required for the platinum drug resistance

To identify a possible resistance-related domain within the annexin repeated sequence of ANXA4, we constructed 3 deletion mutants by deleting the annexin repeats one by one from the C-terminal region. Figure 3A shows the structure of each deletion mutant. Full-length ANXA4, 3 ANXA4 deletion mutants or the empty vector were transfected into NUGC3 cells, whose endogenous ANXA4 expression is relatively low (Supplementary Fig. S1). Therefore, we established cell lines stably overexpressing full-length ANXA4 (FL-22), each ANXA4 deletion mutant (R3-6, R2-13 or R1-12) or the empty vector (NC-14). Expression of each ANXA4 deletion mutant was confirmed using Western blotting (Fig. 3B).

Subsequently, the sensitivity to the platinum-based drugs cisplatin and carboplatin was assessed. Cells transfected with full-length ANXA4 and the 3 deletion ANXA4 mutants were significantly more resistant to both cisplatin and carboplatin compared with control cells, approximately with a 1.7- to 2.2-fold increase in IC_{50} for cisplatin ($p < 0.01$) and a 1.4- to 1.7-fold increase in IC_{50} for carboplatin ($p < 0.05$; Fig. 3C).

To test whether these deletion mutants induce platinum resistance through regulating cellular drug concentration as previously reported [28], we quantitated the intracellular platinum content of each deletion mutant-transfected cell clone after cisplatin treatment, which is one of the most representative platinum drugs. Platinum accumulation was significantly reduced in cells overexpressing either full-length ANXA4 or any of the 3

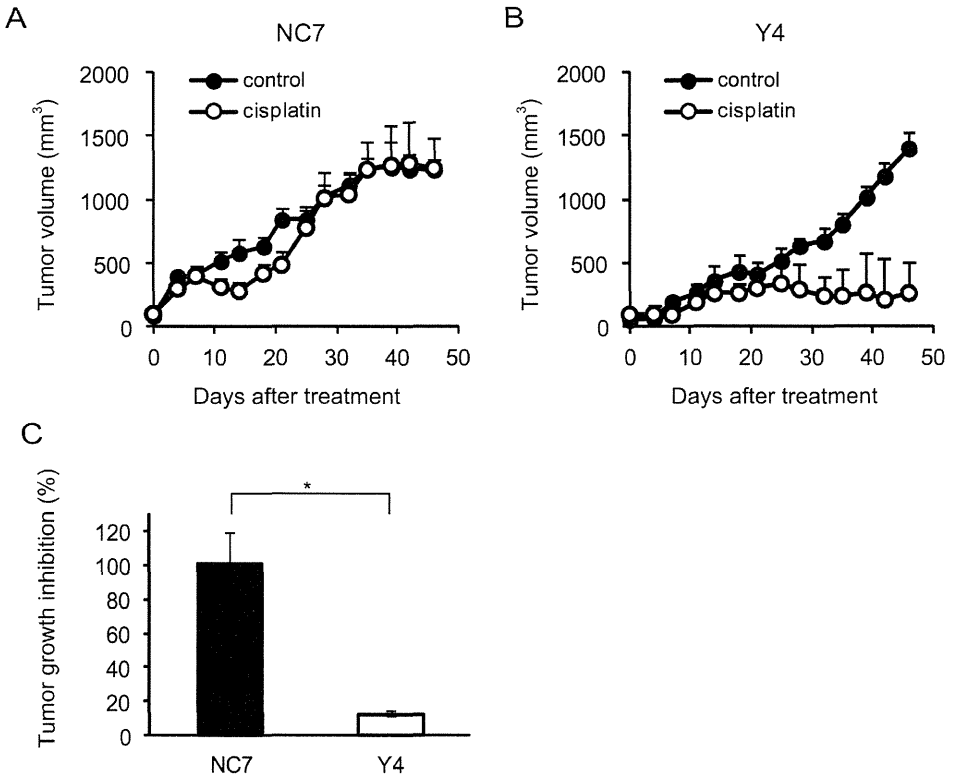

Fig.2: ANXA4 knockdown cells show enhanced sensitivity to cisplatin *in vivo*. Female ICR *nu/nu* mice were subcutaneously inoculated with RMG-I NC7 or Y4 cells and given PBS (control group: *filled circles*) or cisplatin i.p. (3 mg/kg; treatment group: *open circles*) twice weekly for 4 weeks (n = 6 per group). Growth curves of NC7 tumours (A) and Y4 tumours (B). The mean volume (points) ± SE (bars) is shown. (C) Comparison of the cisplatin-induced growth inhibition of tumours 46 days after treatment among NC7 and Y4 tumours. The average (columns) ± SE (bars) are shown (*$p < 0.01$).

deletion mutants compared with NC-14 cells regardless of the incubation time after cisplatin exposure (Fig. 3D). These results suggested that the decreased intracellular platinum contents were associated with platinum resistance of the cells transfected with ANXA4 full length and each deletion mutant.

The calcium-binding site of the annexin repeat is responsible for platinum resistance

As specified above, platinum resistance was enhanced in cells overexpressing ANXA4 deletion mutants, which contained at least 1 intact annexin repeat. Thus, to assess whether the calcium-binding site of the annexin repeat sequence was involved in chemoresistance, another deletion mutant, R1(E70A) was constructed. Within the annexin repeat next to the N-terminal region, the 70th amino acid, glutamic acid, was responsible for the calcium-dependent activity of ANXA4 [30]. Accordingly, at this site, the point mutation variant of R1, R1(E70A), loses the function of its calcium-binding site (Fig. 4A). Similar to other deletion mutants, R1(E70A) was transfected into NUGC3 cells and designated R1(E70A)-95. Western blotting revealed that R1-12 had the same molecular weight as R1(E70A)-95 (Fig. 4B). R1(E70A)-95 did not induce resistance to either cisplatin or carboplatin (Fig. 4C). Moreover, the intracellular platinum content of R1(E70A)-95-transfected cells did not decrease compared with that of NC-14 cells after 0 hr

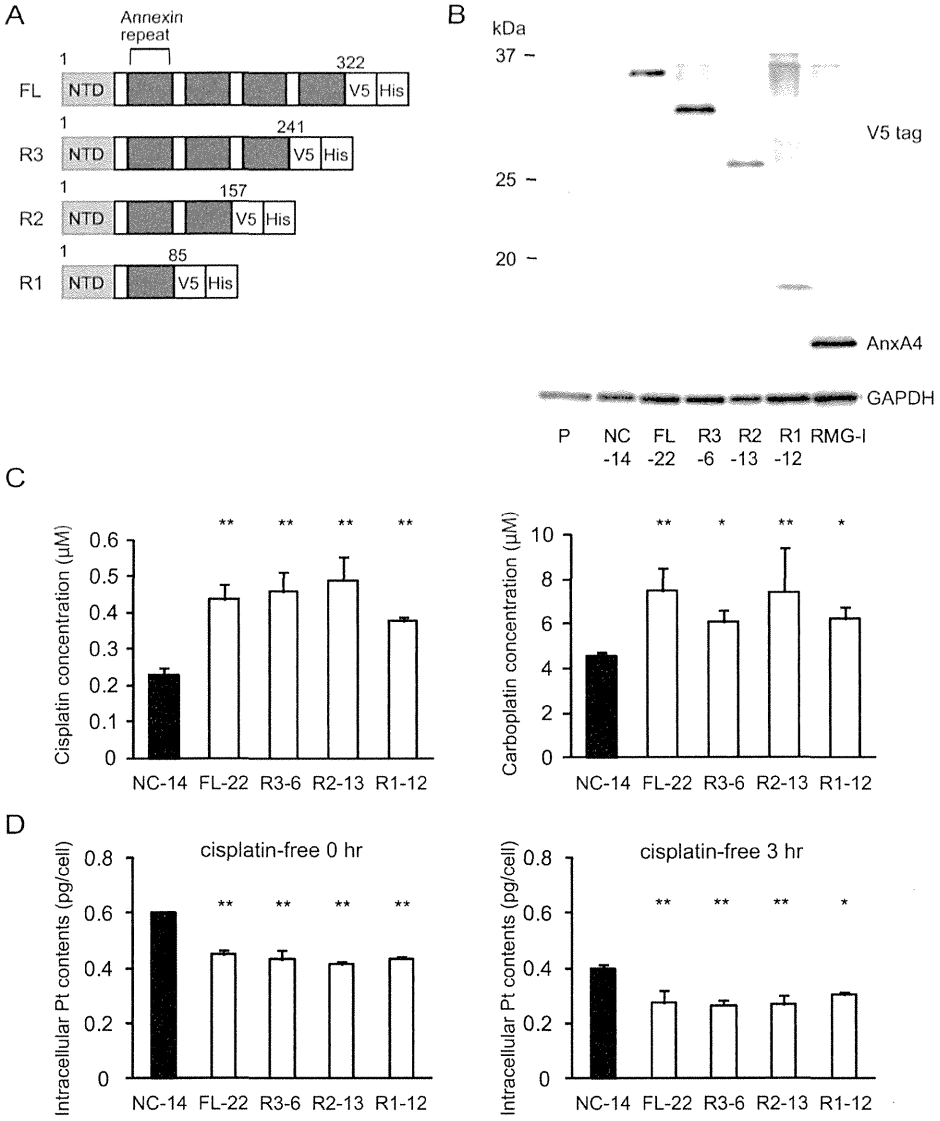

Fig.3: Annexin repeat domain is required for the platinum drug resistance. (A) A structural map of ANXA4 and 3 deletion mutant proteins. Annexin repeats were deleted one by one from the C-terminal site. (B) Established deletion mutant cells together with parent cells, control cells and RMG-I as a positive control were confirmed using Western blotting. (C) Compared with NC-14 cells, IC_{50} for both cisplatin and carboplatin was significantly increased in FL-22 and all other mutant cells. (D) Intracellular platinum accumulation after treatment with 100 μM cisplatin for 60 min with or without additional 3 hr of incubation in cisplatin-free medium. Data are presented as mean ± SD (*$p < 0.05$, **$p < 0.01$).

or 3 hr of additional incubation in cisplatin-free medium (Fig. 4D). According to the above results, the platinum resistance of ANXA4 seemed to be related to the calcium-binding site of the annexin repeat next to the N-terminal domain.

The calcium-binding site of the annexin repeated sequence is required for the resistance to platinum-based drugs *in vivo*

To determine whether the annexin deletion mutants of ANXA4 influenced the sensitivity to cisplatin *in vivo*, we inoculated ICR *nu/nu* mice with NC-14, FL-22, R1-12 or R1(E70A)-95 cells. Mice in each group were randomised into 2 subgroups and received either cisplatin at 3 mg/(kg·d) or PBS *i.p.* once a week for 3 weeks. Cisplatin markedly decreased tumour volume in mice injected with NC-14 and R1(E70A)-95 cells, whereas the treatment effect was relatively smaller in mice injected with FL-22 and R1-12 cells (Fig. 5A). Consistent with the tumour volume, tumour growth was significantly inhibited by cisplatin in mice inoculated with NC-14 (96.5 ± 1.3%) and R1(E70A)-95 cells (87.8 ± 11.4%) compared with those injected with FL-22 (48.5 ± 11.7%) and R1-12 cells (37.7 ± 9.8%; $p < 0.01$; Fig. 5B). These *in vivo* results

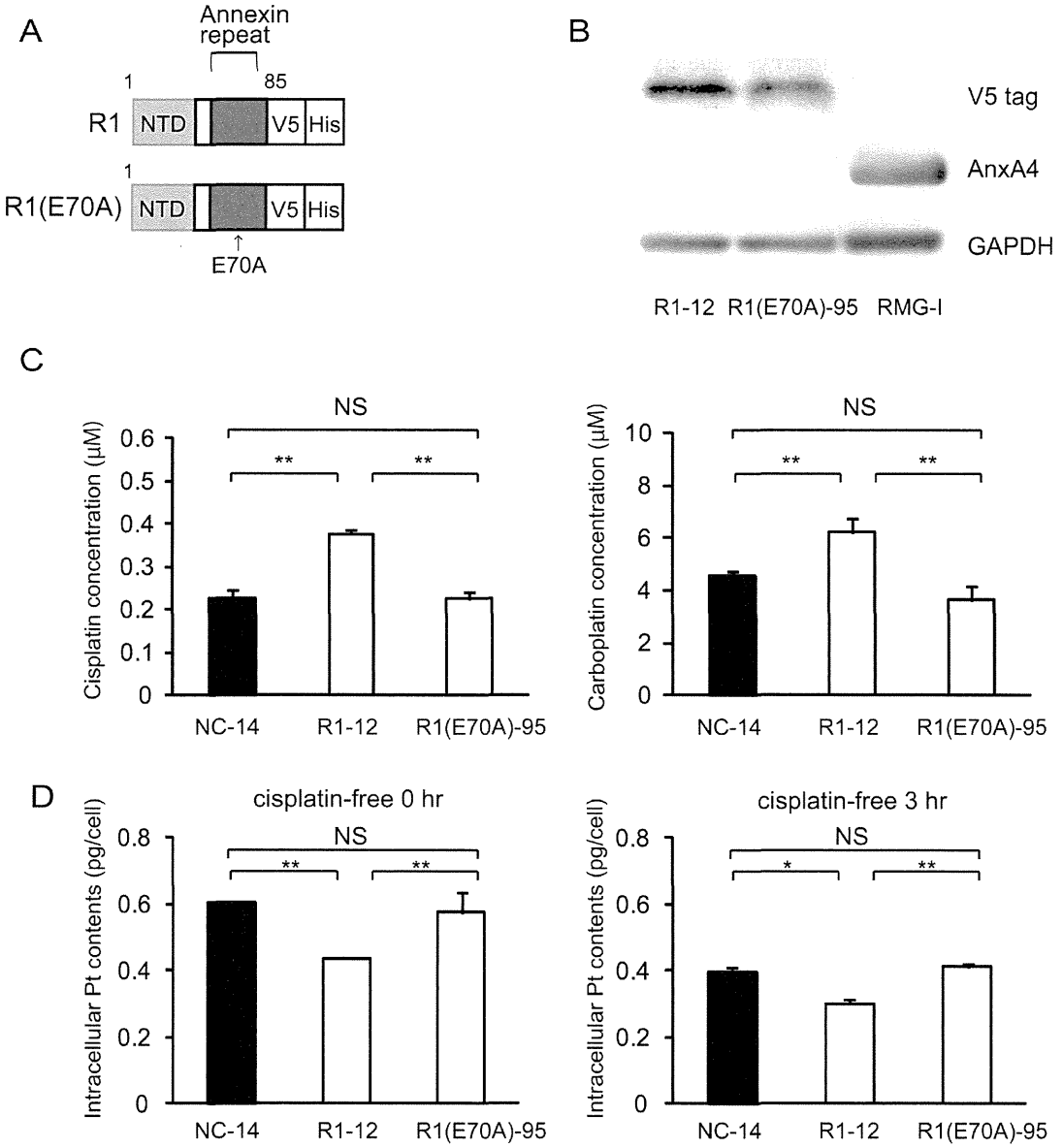

Fig.4: The calcium-binding site of the annexin repeat is responsible for induction of the platinum resistance. (A) A structural map of R1 and R1(E70A) variants without a function for the calcium-binding site. (B) Western blotting confirmed the mutant established cell lines. (C) Unlike R1-12, the R1(E70A)-95 cell clone was not resistant to either cisplatin or carboplatin. (D) Intracellular platinum accumulation in R1(E70A) cells was the same as in NC14 cells both with or without additional 3 hr of incubation in cisplatin-free medium. Data are presented as mean ± SD (*$p < 0.05$, **$p < 0.01$).

were consistent with those obtained *in vitro*.

Increase of the intracellular chloride concentration is related to cisplatin resistance

To elucidate the molecular mechanisms of chemoresistance induced by ANXA4, we focused on the chloride channel because one of the functions of ANXA4 is inhibition of calcium-dependent chloride conductance[32]. According to the literature, treatment with cisplatin induces an increase of the intracellular Ca^{2+} concentration [46], which is an important ion for the phospholipid membrane-binding activity of ANXA4. In contrast, cisplatin exposure also induces an elevation of the intracellular chloride concentration: $[Cl^-]_i$ [47]. Elevation of $[Cl^-]_i$ has been shown to prevent the aquation of 1 or 2 of the 2 chloride coordination sites in cisplatin, and only the aquated forms of cisplatin covalently bind to DNA. Nevertheless, the mechanisms of $[Cl^-]_i$ elevation because of cisplatin treatment have not been fully elucidated. We hypothesised that an increase in intracellular Ca^{2+} concentration after cisplatin exposure would result in translocation of ANXA4 from the cytosol to plasma membrane, which leads to $[Cl^-]_i$ accumulation through inhibition of the chloride channel by the Ca^{2+}-bound ANXA4. To confirm this hypothesis, we quantified $[Cl^-]_i$ after cisplatin treatment using MAQE fluorescence, a fluorescent Cl^- indicator. Relative fluorescence was substituted for $[Cl^-]_i$ as previously reported [48].

We monitored MQAE fluorescence in control cells (NC-14), in cells overexpressing full-length ANXA4 (FL-22) and in 2 deletion mutants (R1-12 and R1[E70A]-95). The relative fluorescence ratio before (F0) and after

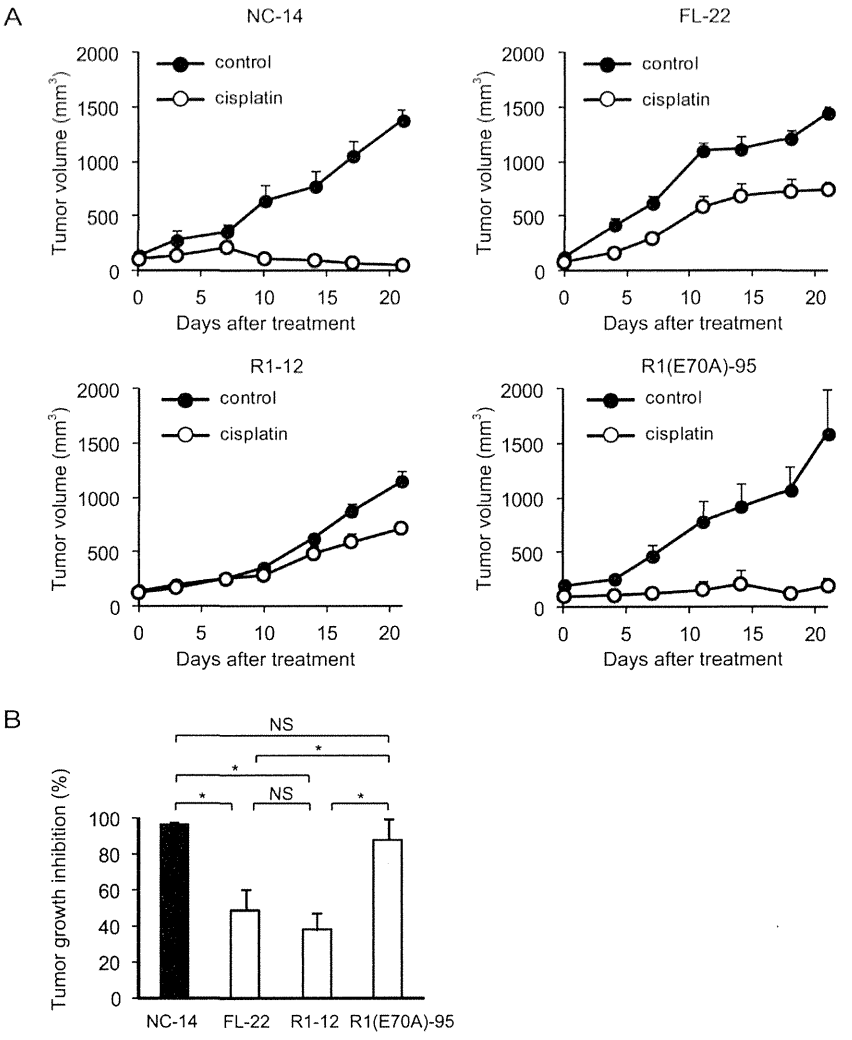

Fig.5: The calcium-binding site of the annexin repeat is required for platinum drug resistance *in vivo*. Female ICR *nu/nu* mice were subcutaneously inoculated with NC14, FL-22, R1-12 or R1(E70A)-95 cells and given PBS (control group: *filled circles*) or cisplatin i.p. (3 mg/kg; treatment group: *open circles*) once a week for 3 weeks (n = 6 per group). (A) Growth curves of tumours of each cell. The mean volume (points) ± SE (bars) is shown. (B) Comparison of the cisplatin-induced growth inhibition of tumours 28 days after treatment. The average (columns) ± SE (bars) are shown; $*p < 0.01$.

treatment with cisplatin for 30 min (F30) is shown in Figure 6. The inverse ratio of MQAE fluorescence 1/(F30/F0), which is directly proportional to the increase in $[Cl^-]_i$, was significantly elevated in the platinum-resistant cell clones FL-22 (1.12 ± 0.03) and R1-12 (1.12 ± 0.01) compared with sensitive clones, NC-14 (1.06 ± 0.01) and R1(E70A)-95 (1.06 ± 0.02; $p < 0.01$). Thus, the increase in $[Cl^-]_i$ is likely to be involved in cisplatin resistance.

DISCUSSION

ANXA4 has been reported to be strongly expressed and involved in chemoresistance in various cancers. The factors associated with ANXA4-induced chemoresistance have been reported, such as NF-κB [45] and ATP7A [44], but the structure of the protein, i.e. annexin repeats and calcium-binding sites in the annexin repeated sequence, has not been taken into account in relation to the ANXA4-induced chemoresistance. In this study, we showed that ANXA4 knockdown improved sensitivity to platinum drugs, and annexin repeats were involved in chemoresistance.

We first confirmed ANXA4 expression in various ovarian adenocarcinoma cell lines. As previously reported [28, 49], ANXA4 is significantly upregulated in clear cell carcinoma cell lines (OVTOKO, OVISE and RMG-I) compared with other histological types (serous and mucinous adenocarcinoma cell lines: A2780, OVCAR3, OVSAHO and MCAS). It has been previously demonstrated that enhanced ANXA4 expression induces platinum resistance both *in vitro* and *in vivo* [28, 44], but whether ANXA4 knockdown attenuates platinum resistance has been unknown thus far. Mogami et al. recently reported that an ANXA4 knockdown improves sensitivity to carboplatin *in vitro* using 2 cell lines of ovarian clear cell carcinoma, OVTOKO and OVISE. To the best of our knowledge, ours is the first study to show that ANXA4 knockdown markedly improves the sensitivity to platinum-based drugs not only *in vitro* but also *in vivo* (Figs. 1 and 2).

The result that ANXA4 knockdown improves sensitivity to platinum-based drugs suggests that ANXA4 is a good therapeutic target. To identify the functional domain(s) of ANXA4 that could be a promising therapeutic target, we focused on annexin repeats and constructed 4 deletion mutants (R3, R2, R1 and R1[E70A]). Resistance to platinum drugs was enhanced in cells transfected with mutants possessing at least 1 intact annexin repeat. In contrast, the sensitivity to platinum-based drugs improved among the R1(E70A)-transfected clones because in those cells, the calcium-binding site did not function properly (Figs. 3C and 4C). This result implies that the ANXA4-induced chemoresistance to platinum-based agents is calcium dependent. It has been reported that cisplatin induced increase of intracellular calcium concentration in chemosensitive cells, but not in resistant cells [46, 50]. Together with this and the data by Chan et al., elevation of intracellular calcium concentration induced by cisplatin treatment may translocate Ca^{2+} bound form of ANXA4 from cytosol to plasma membrane, which results in platinum-resistance[32]. We are currently investigating on further analysis.

By analysing the intracellular platinum accumulation, we attempted to elucidate the mechanism of the platinum resistance induced by ANXA4 and its deletion mutants. When intracellular platinum contents were quantitated just after exposure to cisplatin or 3 hr incubation with cisplatin-free medium after exposure to cisplatin, significantly less platinum accumulated in cells transfected with the full-length ANXA4 (FL-22) and 3 deletion mutants (R3-6, R2-13 and R1-12), all of which enhanced the resistance to the platinum-based drugs. In contrast, R1(E70A)-transfected cells (R1[E70A]-95), which did not induce chemoresistance, had the same amount of platinum accumulation as the control cells (Figs. 3D and 4D). These results suggest that the resistance to the platinum-based drugs is mediated by the decrease in intracellular platinum accumulation, which is calcium dependent. The annexin repeats, especially their calcium-binding sites, may be involved in inhibition of the influx, promotion of the efflux or both of platinum drugs. Recently, Cu transporters (CTR1 for the uptake and ATP7A and ATP7B for the efflux) have been reported to be involved in resistance to both cisplatin and carboplatin [14, 44, 51]. In addition, ANXA4 likely enhance platinum efflux through the interaction with ATP7A [44]. The possible mechanisms of inhibition of the influx mediated by ANXA4 remains unclear and further analyses are needed.

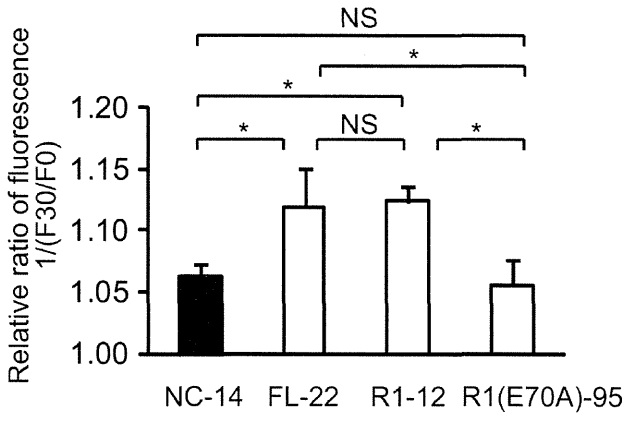

Fig.6: The increase of intracellular chloride concentration is related to cisplatin resistance. ANXA4 deletion mutant series cells (NC-14, FL-22, R1-12 and R1[E70A]-95) loaded with N-ethroxycarbonymethyl-6-methoxyquinolinium bromide (MQAE) were exposed to 100 μM cisplatin. The fluorescence pre-treatment and during treatment (30 min exposure) was compared in each cell clone. Data are presented as mean ± SD (*$p < 0.01$).

Subsequently, the question regarding the involvement of calcium-binding site in the platinum resistance arose. To answer this question, we measured $[Cl^-]_i$ after cisplatin exposure. The significant increase in $[Cl^-]_i$ was observed in the cells with platinum resistance, FL-22 and R1-12, compared with cell clones without platinum resistance, NC-14 and R1(E70A)-95. In a previous study, higher $[Cl^-]_i$ was observed in cisplatin-resistant cells compared with sensitive cells, whereas the intracellular cisplatin accumulation showed the opposite pattern [47]. These results, in addition to the results of decreased platinum accumulation in resistant mutants, indicate that ANXA4 induces platinum resistance through cellular drug efflux partly by elevating the intracellular chloride concentration. We report 'partly' because only cisplatin, not carboplatin, was tested in our $[Cl^-]_i$ assay. Cisplatin becomes intracellularly activated by the aquation of 1 or 2 of the 2 chloride coordination sites, but carboplatin does not contain any chloride coordination sites [1, 52-54]. Thus, this mechanism of resistance through elevation of $[Cl^-]_i$ may be specific to cisplatin and may not be true of carboplatin resistance. In this study, 3 cell clones overexpressing a deletion mutant (R3-6, R2-13, and R1-12) show stronger tolerance to cisplatin than to carboplatin in terms of their IC_{50}: a 1.7- to 2.2-fold increase for cisplatin and only a 1.4- to 1.7-fold increase for carboplatin (Fig. 3C). It is assumed that the increase in $[Cl^-]_i$ is one of the factors inducing cisplatin resistance.

In this study, the calcium-binding site in the annexin repeat next to the N terminus was observed to be responsible for the resistance to the platinum drugs. Nevertheless, the role of the other 3 calcium-binding sites has not yet been investigated. The roles of individual calcium-binding sites were demonstrated using site-directed mutagenesis by Nelson and Creutz regarding calcium-dependent membrane binding and aggregation [30]. The mutations in each domain had different effects on the binding or aggregating activities, i.e. a mutation in the first or fourth domain had a greater effect on membrane binding. A mutation in the second domain had a stronger effect on membrane aggregation, whereas the mutation of the third domain was almost silent. Although the mechanisms involved in membrane binding/aggregation and the mechanisms of chemoresistance are likely different, our data could provide some clues to understanding the function of each annexin repeat and each calcium-binding site in chemoresistance.

ANXA4 has been shown to induce resistance to paclitaxel and platinum-based drugs [55]. The effect of ANXA4 knockdown on paclitaxel sensitivity was assessed in a previous study. The effect of sensitivity to paclitaxel varied among different cell clones: ANXA4 knockdown in the OVTOKO cell line with acidic isoelectric point (IEPs) did not improve the sensitivity to paclitaxel, whereas OVISE cell lines with basic IEPs showed improved sensitivity to paclitaxel [43]. In our own preliminary data, significant chemosensitisation to paclitaxel and etoposide was confirmed in RMG-I Y4 and R5 (data not shown). Further studies are required to identify the detailed mechanism.

In summary, in this study, we observed the annexin repeat, especially its calcium binding site, was associated with platinum-resistance induced by ANXA4, and it happened in calcium-dependent manner. Our findings may help to understand the mechanisms of platinum resistance induced by other annexin family proteins, which possesses the same annexin repeat structure, and offer new strategies for the treatment of chemoresistant cancers.

METHODS

Cell lines and culture

The human ovarian serous adenocarcinoma cell line (OVSAHO), human ovarian mucinous adenocarcinoma cell line (MCAS), human ovarian clear cell carcinoma cell lines (OVTOKO, OVISE and RMG-I) and human gastric cancer cell line (NUGC3) were obtained from the Japanese Collection of Research Bioresources (Osaka, Japan). A2780 cells from the human ovarian serous adenocarcinoma were obtained from the European Collection of Animal Cell Culture (Salisbury, Scotland) and OVCAR-3 cells from another human ovarian serous adenocarcinoma were from American Type Culture Collection (Manassas, VA). MCAS cells were maintained in the DMEM medium and the others in the RPMI medium, all supplemented with 10% foetal bovine serum (FBS; Serum Source International, NC, USA) and 1% penicillin–streptomycin (Nacalai Tesque, Kyoto, Japan) at 37°C in a humidified atmosphere with 5% CO_2. All the cell lines were tested and authenticated.

Generation of ANXA4 knockdown cell lines

To generate stable ANXA4 knockdown cell lines, RMG-I cells were transfected with a commercial plasmid vector expressing short heparin RNA (shRNA) that targeted ANXA4 mRNA or a negative control nonspecific shRNA (SuperArray Bioscience Corp., KH06928N; Frederick, MD, USA) using Lipofectamine 2000 (Invitrogen, Carlsbad, CA), according to the manufacturer's instructions. After selection using a culture medium containing geneticin (600 μg/mL; Invitrogen), stable clones were maintained in 250 μg/mL geneticin. Two stable RMG-I-ANXA4 shRNA cell clones were established, designated Y4 and R5 cells. In addition, we transfected the empty vector into the RMG-I cell line using the same procedure to generate control cells, designated NC7.

Construction of ANXA4 deletion mutants and gene transfection

Using pcDNA3.1-ANXA4 as a template, full-length cDNA of ANXA4 was amplified using KOD-plus (Toyobo Co. Led., Osaka, Japan) with the primers forward 5′-TTGACCTAGAGTCATGGCCA-3′, reverse 5′-ATCATCTCCTCCACAGAGAA-3′ and subsequently ligated into the pcDNA3.1/V5-His-TOPO vector in-frame with the C-terminal V5 and 6× His tag. To generate ANXA4 deletion mutants, annexin repeat domains were deleted one by one from the C-terminal site. Three deletion mutants named R3, R2 and R1 were generated and similarly amplified (an Arabic number shows the number of annexin repeat domains). The nucleotide sequences of the forward primers for PCR were the same as those described above for all the deletion mutants, and the reverse primers were as follows: R3 5′-TATAGCCAGCAGAGCATCTT-3′, R2 5-CAGAGACACCAGCACTCGCT-3′ and R1 5′-CATCCCCACAATCACCTGCT-3′. We subsequently set out to generate an R1 mutant (the E70A mutation), whose calcium-binding site does not work because of the change of a negatively charged carboxyl group to a neutral side chain, as previously described [30]. The site-directed mutagenesis was performed using the KOD-Plus-Mutagenesis kit (Toyobo), according to the manufacturer's protocol. These cDNA fragments, including full-length gene, were subsequently inserted between the *Bgl* II and *EcoR* I sites of the pIRES2AcGFP vector (Clontech, Palo Alto, CA). The sequences of all the mutants were confirmed using the ABI PRISM 3100 Genetic Analyser (Applied Biosystems, Foster City, USA).

Full-length ANXA4, each ANXA4 deletion mutant construct and the empty vector were transfected into NUGC3 cells using Lipofectamine 2000 (Invitrogen). Stable transfectants designated FL-12, R3-6, R2-13, R1-12, R1(R70A)-95 and NC-14 were obtained by selection in a medium containing geneticin and were maintained in the same manner described above.

Western blotting

Cells were lysed in RIPA buffer (10 mM Tris–HCl, pH 7.5, 150 mM NaCl, 1% Nonidet P-40, 0.1% sodium deoxycholate, 0.1% SDS, 1× phosphatase inhibitor cocktail (Nacalai Tesque) and 1× protease inhibitor cocktail (Nacalai Tesque)), followed by centrifugation (13,200 rpm, 4°C, 15 min). Soluble proteins in the supernatant were separated using sodium dodecyl sulphate polyacrylamide gel electrophoresis, as described previously [28]. Additional information can be found in the Supporting Information on Material and Methods section.

Measurement of IC_{50} values after treatment with a platinum-based drug

Cells were suspended in the RPMI medium supplemented with 10% FBS, seeded in 96-well plates (1,500/well for the RMG-I series and 2,500 cells/well for ANXA4 deletion mutant series), cultured for 24 h and exposed to various concentrations of cisplatin (0–25 μM; Sigma–Aldrich, St Louis, MO) or carboplatin (0–1000 μM; Sigma–Aldrich) for 72 h. Cellular proliferation was subsequently evaluated using the WST-8 assay, i.e. 2-(2-methyosy-4-nitro-phenyl)-3-(4-nitrophenyl)-5-(2,4-disulfophynel)-2H-tetrazolium monosodium salt assay (Cell Counting Kit-SF; Nacalai Tesque) after treatment. The absorption of WST-8 was measured at a wavelength of 450 nm (reference wavelength: 630 nm) using a Model 680 microplate reader (Bio-Rad Laboratories, Hercules, CA). Absorbance values for the treated samples were expressed as percentages relative to results for untreated controls, and IC_{50} values were calculated.

Measurement of intracellular platinum accumulation

Full-length ANXA4-transfected cells (FL-22), each ANXA4 deletion mutant-transfected cell clone (R3-6, R2-13, R1-12 and R1[E70A]-95), and control cells (NC-14) were cultured up to 80% confluence in 150-mm tissue culture dishes. The cells were then exposed to 100 μM cisplatin for 60 min at 37°C and washed twice with PBS either immediately or after 3 hr of incubation in cisplatin-free RPMI 1640 medium supplemented with 10% FBS. Whole-cell extracts were prepared, and the concentration of intracellular platinum was determined using an Agilent 7500ce inductively coupled plasma mass spectrometer (ICP-MS; Agilent, Santa Clara, CA, USA).

In vivo model of cisplatin resistance

All animal experiments were conducted in accordance with the Institutional Ethical Guidelines for Animal Experimentation of the National Institute of Biomedical Innovation (Osaka, Japan). Female Institute of Cancer Research (ICR) *nu/nu* mice were obtained from Charles River Japan (Yokohama, Japan). Injection of the ANXA4 knockdown cells was performed as follows: ICR *nu/nu* mice at 4 weeks of age were subcutaneously inoculated (into the flank of the mice; n = 6 per group) with 2.5 × 10^6 cells of RMG-I NC7 cells or RMG-I-Y4 cells in the total volume of 100 μL of 1/1 (v/v) PBS/Matrigel (Becton Dickinson, Bedford, MA). Injection of ANXA4 mutant-transfected cells, i.e. mice at 5 weeks of age were inoculated with 10^6 cells of NC-14, FL-22, R1-12 or R1(E70A) in the same manner

as with the ANXA4 knockdown cells. Treatment with cisplatin (3 mg/kg) or PBS *i.p.* was initiated 1 week after inoculation and administered twice weekly for 4 weeks (ANXA4 knockdown cells) and once a week for 3 weeks (ANXA4 mutant-transfected cells). Tumour volumes were determined twice weekly by measuring length (L), width (W) and depth (D) and using the following formula: tumour volume (mm^3) = W × L × D.

$[Cl^-]_i$ measurements

$[Cl^-]_i$ was measured using the fluorescent Cl^- indicator N-ethroxycarbonymethyl-6-methoxyquinolinium bromide (MQAE; Dojindo, Kumamoto, Japan). $[Cl^-]_i$ is detected by the mechanism of diffusion-limited collisional quenching of MQAE fluorescence. MQAE fluorescence intensity inversely correlates with $[Cl^-]_i$. The cells of the ANXA4 deletion mutant series (NC-14, FL-22, R1-12 and R1[E70A]-95) were cultured in 35-mm tissue culture dishes up to 20% confluence and incubated with a medium containing 10 mM MQAE for 4 h at 37°C. After loading, the cells were washed 5 times with Cl^--free buffer and electrically stimulated under a microscope at 37°C in a humidified atmosphere with 5% CO_2. Fluorescence measurements were initiated immediately at the indicated periods using Biozero BZ-9000 (Keyence, Tokyo, Japan) at 510/40 nm excitation and 380/50 nm emission. The fluorescence was quantitated by means of a standardised procedure using a BZ-II Analyser (Keyence), and the data were presented as the reciprocal of the ratio of fluorescence data (F0/F30) to identify possible correlations with the increase in $[Cl^-]_i$.

Statistical analysis

All calculations involved one-way analysis of variance (ANOVA) followed by Dunnett's analysis to evaluate the significance of differences. In all experiments, p value of <0.05 was considered statistically significant.

ACKNOWLEDGEMENTS

We thank Y. Kanazawa and A. Yagi for their secretarial assistance, M. Ako and E. Harada for technical assistance.

There are no conflicts of interest to declare. This study was supported by a Grant-in-Aid from the Program for Promotion of Fundamental Studies in Health Sciences of the National Institute of Biomedical Innovation; a Grant-in-Aid from the Ministry of Health, Labour and Welfare of Japan and Grants-in-Aid for Young Scientists (B) (22791560) from the Japanese Ministry of Education, Science, Culture and Sports

REFERENCES

1. Kelland L. The resurgence of platinum-based cancer chemotherapy. Nat Rev Cancer. 2007; 7(8):573-584.
2. Loriot Y, Mordant P, Deutsch E, Olaussen KA and Soria JC. Are RAS mutations predictive markers of resistance to standard chemotherapy? Nat Rev Clin Oncol. 2009; 6(9):528-534.
3. Alva AS, Matin SF, Lerner SP and Siefker-Radtke AO. Perioperative chemotherapy for upper tract urothelial cancer. Nat Rev Urol. 2012; 9(5):266-273.
4. Bookman MA. First-line chemotherapy in epithelial ovarian cancer. Clin Obstet Gynecol. 2012; 55(1):96-113.
5. Matos CS, de Carvalho AL, Lopes RP and Marques MP. New strategies against prostate cancer--Pt(II)-based chemotherapy. Curr Med Chem. 2012; 19(27):4678-4687.
6. Rossi A, Di Maio M, Chiodini P, Rudd RM, Okamoto H, Skarlos DV, Fruh M, Qian W, Tamura T, Samantas E, Shibata T, Perrone F, Gallo C, Gridelli C, Martelli O and Lee SM. Carboplatin- or cisplatin-based chemotherapy in first-line treatment of small-cell lung cancer: the COCIS meta-analysis of individual patient data. J Clin Oncol. 2012; 30(14):1692-1698.
7. Muggia FM and Los G. Platinum resistance: laboratory findings and clinical implications. Stem Cells. 1993; 11(3):182-193.
8. Jassem J. Chemotherapy of advanced non-small cell lung cancer. Ann Oncol. 1999; 10 Suppl 6:77-82.
9. Perez RP. Cellular and molecular determinants of cisplatin resistance. Eur J Cancer. 1998; 34(10):1535-1542.
10. Fuertes MA, Castilla J, Alonso C and Perez JM. Novel concepts in the development of platinum antitumor drugs. Curr Med Chem Anticancer Agents. 2002; 2(4):539-551.
11. Gonzalez VM, Fuertes MA, Alonso C and Perez JM. Is cisplatin-induced cell death always produced by apoptosis? Mol Pharmacol. 2001; 59(4):657-663.
12. Niedner H, Christen R, Lin X, Kondo A and Howell SB. Identification of genes that mediate sensitivity to cisplatin. Mol Pharmacol. 2001; 60(6):1153-1160.
13. Ishida S, Lee J, Thiele DJ and Herskowitz I. Uptake of the anticancer drug cisplatin mediated by the copper transporter Ctr1 in yeast and mammals. Proc Natl Acad Sci U S A. 2002; 99(22):14298-14302.
14. Safaei R, Holzer AK, Katano K, Samimi G and Howell SB. The role of copper transporters in the development of resistance to Pt drugs. J Inorg Biochem. 2004; 98(10):1607-1613.
15. Katano K, Kondo A, Safaei R, Holzer A, Samimi G, Mishima M, Kuo YM, Rochdi M and Howell SB. Acquisition of resistance to cisplatin is accompanied by changes in the cellular pharmacology of copper. Cancer Res. 2002; 62(22):6559-6565.
16. Samimi G, Varki NM, Wilczynski S, Safaei R, Alberts DS and Howell SB. Increase in expression of the copper

transporter ATP7A during platinum drug-based treatment is associated with poor survival in ovarian cancer patients. Clin Cancer Res. 2003; 9(16 Pt 1):5853-5859.

17. Rabik CA, Maryon EB, Kasza K, Shafer JT, Bartnik CM and Dolan ME. Role of copper transporters in resistance to platinating agents. Cancer Chemother Pharmacol. 2009; 64(1):133-142.
18. Koike K, Kawabe T, Tanaka T, Toh S, Uchiumi T, Wada M, Akiyama S, Ono M and Kuwano M. A canalicular multispecific organic anion transporter (cMOAT) antisense cDNA enhances drug sensitivity in human hepatic cancer cells. Cancer Res. 1997; 57(24):5475-5479.
19. Cui Y, Konig J, Buchholz JK, Spring H, Leier I and Keppler D. Drug resistance and ATP-dependent conjugate transport mediated by the apical multidrug resistance protein, MRP2, permanently expressed in human and canine cells. Mol Pharmacol. 1999; 55(5):929-937.
20. Liedert B, Materna V, Schadendorf D, Thomale J and Lage H. Overexpression of cMOAT (MRP2/ABCC2) is associated with decreased formation of platinum-DNA adducts and decreased G2-arrest in melanoma cells resistant to cisplatin. J Invest Dermatol. 2003; 121(1):172-176.
21. Ban N, Takahashi Y, Takayama T, Kura T, Katahira T, Sakamaki S and Niitsu Y. Transfection of glutathione S-transferase (GST)-pi antisense complementary DNA increases the sensitivity of a colon cancer cell line to adriamycin, cisplatin, melphalan, and etoposide. Cancer Res. 1996; 56(15):3577-3582.
22. Olaussen KA, Dunant A, Fouret P, Brambilla E, Andre F, Haddad V, Taranchon E, Filipits M, Pirker R, Popper HH, Stahel R, Sabatier L, Pignon JP, Tursz T, Le Chevalier T and Soria JC. DNA repair by ERCC1 in non-small-cell lung cancer and cisplatin-based adjuvant chemotherapy. N Engl J Med. 2006; 355(10):983-991.
23. Wang Q, Shi S, He W, Padilla MT, Zhang L, Wang X, Zhang B and Lin Y. Retaining MKP1 expression and attenuating JNK-mediated apoptosis by RIP1 for cisplatin resistance through miR-940 inhibition. Oncotarget. 2014; 5(5):1304-1314.
24. Li H and Yang BB. MicroRNA in drug resistance. Oncoscience. 2014; 1(1):2.
25. Yang H, Kong W, He L, Zhao JJ, O'Donnell JD, Wang J, Wenham RM, Coppola D, Kruk PA, Nicosia SV and Cheng JQ. MicroRNA expression profiling in human ovarian cancer: miR-214 induces cell survival and cisplatin resistance by targeting PTEN. Cancer Res. 2008; 68(2):425-433.
26. Sorrentino A, Liu CG, Addario A, Peschle C, Scambia G and Ferlini C. Role of microRNAs in drug-resistant ovarian cancer cells. Gynecol Oncol. 2008; 111(3):478-486.
27. Perego P, Giarola M, Righetti SC, Supino R, Caserini C, Delia D, Pierotti MA, Miyashita T, Reed JC and Zunino F. Association between cisplatin resistance and mutation of p53 gene and reduced bax expression in ovarian carcinoma cell systems. Cancer Res. 1996; 56(3):556-562.
28. Kim A, Enomoto T, Serada S, Ueda Y, Takahashi T, Ripley B, Miyatake T, Fujita M, Lee CM, Morimoto K, Fujimoto M, Kimura T and Naka T. Enhanced expression of Annexin A4 in clear cell carcinoma of the ovary and its association with chemoresistance to carboplatin. Int J Cancer. 2009; 125(10):2316-2322.
29. Gerke V and Moss SE. Annexins: from structure to function. Physiol Rev. 2002; 82(2):331-371.
30. Nelson MR and Creutz CE. Combinatorial mutagenesis of the four domains of annexin IV: effects on chromaffin granule binding and aggregating activities. Biochemistry. 1995; 34(9):3121-3132.
31. Kaetzel MA, Hazarika P and Dedman JR. Differential tissue expression of three 35-kDa annexin calcium-dependent phospholipid-binding proteins. J Biol Chem. 1989; 264(24):14463-14470.
32. Chan HC, Kaetzel MA, Gotter AL, Dedman JR and Nelson DJ. Annexin IV inhibits calmodulin-dependent protein kinase II-activated chloride conductance. A novel mechanism for ion channel regulation. J Biol Chem. 1994; 269(51):32464-32468.
33. Kaetzel MA, Mo YD, Mealy TR, Campos B, Bergsma-Schutter W, Brisson A, Dedman JR and Seaton BA. Phosphorylation mutants elucidate the mechanism of annexin IV-mediated membrane aggregation. Biochemistry. 2001; 40(13):4192-4199.
34. Dreier R, Schmid KW, Gerke V and Riehemann K. Differential expression of annexins I, II and IV in human tissues: an immunohistochemical study. Histochem Cell Biol. 1998; 110(2):137-148.
35. Wei R, Zhang Y, Shen L, Jiang W, Li C, Zhong M, Xie Y, Yang D, He L and Zhou Q. Comparative proteomic and radiobiological analyses in human lung adenocarcinoma cells. Mol Cell Biochem. 2012; 359(1-2):151-159.
36. Alfonso P, Canamero M, Fernandez-Carbonie F, Nunez A and Casal JI. Proteome analysis of membrane fractions in colorectal carcinomas by using 2D-DIGE saturation labeling. J Proteome Res. 2008; 7(10):4247-4255.
37. Zimmermann U, Balabanov S, Giebel J, Teller S, Junker H, Schmoll D, Protzel C, Scharf C, Kleist B and Walther R. Increased expression and altered location of annexin IV in renal clear cell carcinoma: a possible role in tumour dissemination. Cancer Lett. 2004; 209(1):111-118.
38. Sitek B, Luttges J, Marcus K, Kloppel G, Schmiegel W, Meyer HE, Hahn SA and Stuhler K. Application of fluorescence difference gel electrophoresis saturation labelling for the analysis of microdissected precursor lesions of pancreatic ductal adenocarcinoma. Proteomics. 2005; 5(10):2665-2679.
39. Xin W, Rhodes DR, Ingold C, Chinnaiyan AM and Rubin MA. Dysregulation of the annexin family protein family is associated with prostate cancer progression. Am J Pathol. 2003; 162(1):255-261.

40. Duncan R, Carpenter B, Main LC, Telfer C and Murray GI. Characterisation and protein expression profiling of annexins in colorectal cancer. Br J Cancer. 2008; 98(2):426-433.
41. Yamashita T, Nagano K, Kanasaki S, Maeda Y, Furuya T, Inoue M, Nabeshi H, Yoshikawa T, Yoshioka Y, Itoh N, Abe Y, Kamada H, Tsutsumi Y and Tsunoda S. Annexin A4 is a possible biomarker for cisplatin susceptibility of malignant mesothelioma cells. Biochem Biophys Res Commun. 2012; 421(1):140-144.
42. Choi CH, Sung CO, Kim HJ, Lee YY, Song SY, Song T, Kim J, Kim TJ, Lee JW, Bae DS and Kim BG. Overexpression of annexin A4 is associated with chemoresistance in papillary serous adenocarcinoma of the ovary. Hum Pathol. 2013; 44(6):1017-1023.
43. Mogami T, Yokota N, Asai-Sato M, Yamada R, Koizume S, Sakuma Y, Yoshihara M, Nakamura Y, Takano Y, Hirahara F, Miyagi Y and Miyagi E. Annexin a4 is involved in proliferation, chemo-resistance and migration and invasion in ovarian clear cell adenocarcinoma cells. PLoS One. 2013; 8(11):e80359.
44. Matsuzaki S, Enomoto T, Serada S, Yoshino K, Nagamori S, Morimoto A, Yokoyama T, Kim A, Kimura T, Ueda Y, Fujita M, Fujimoto M, Kanai Y and Naka T. Annexin A4-conferred platinum resistance is mediated by the copper transporter ATP7A. Int J Cancer. 2013.
45. Jeon YJ, Kim DH, Jung H, Chung SJ, Chi SW, Cho S, Lee SC, Park BC, Park SG and Bae KH. Annexin A4 interacts with the NF-kappaB p50 subunit and modulates NF-kappaB transcriptional activity in a Ca2+-dependent manner. Cell Mol Life Sci. 2010; 67(13):2271-2281.
46. Al-Bahlani S, Fraser M, Wong AY, Sayan BS, Bergeron R, Melino G and Tsang BK. P73 regulates cisplatin-induced apoptosis in ovarian cancer cells via a calcium/calpain-dependent mechanism. Oncogene. 2011; 30(41):4219-4230.
47. Salerno M, Yahia D, Dzamitika S, de Vries E, Pereira-Maia E and Garnier-Suillerot A. Impact of intracellular chloride concentration on cisplatin accumulation in sensitive and resistant GLC4 cells. J Biol Inorg Chem. 2009; 14(1):123-132.
48. Chao AC, Dix JA, Sellers MC and Verkman AS. Fluorescence measurement of chloride transport in monolayer cultured cells. Mechanisms of chloride transport in fibroblasts. Biophys J. 1989; 56(6):1071-1081.
49. Masuishi Y, Arakawa N, Kawasaki H, Miyagi E, Hirahara F and Hirano H. Wild-type p53 enhances annexin IV gene expression in ovarian clear cell adenocarcinoma. FEBS J. 2011; 278(9):1470-1483.
50. Splettstoesser F, Florea AM and Busselberg D. IP(3) receptor antagonist, 2-APB, attenuates cisplatin induced Ca2+-influx in HeLa-S3 cells and prevents activation of calpain and induction of apoptosis. Br J Pharmacol. 2007; 151(8):1176-1186.
51. Safaei R. Role of copper transporters in the uptake and efflux of platinum containing drugs. Cancer Lett. 2006; 234(1):34-39.
52. El-Khateeb M, Appleton TG, Charles BG and Gahan LR. Development of HPLC conditions for valid determination of hydrolysis products of cisplatin. J Pharm Sci. 1999; 88(3):319-326.
53. Kelland LR. Preclinical perspectives on platinum resistance. Drugs. 2000; 59 Suppl 4:1-8; discussion 37-38.
54. Siddik ZH. Cisplatin: mode of cytotoxic action and molecular basis of resistance. Oncogene. 2003; 22(47):7265-7279.
55. Gaudio E, Paduano F, Spizzo R, Ngankeu A, Zanesi N, Gaspari M, Ortuso F, Lovat F, Rock J, Hill GA, Kaou M, Cuda G, Aqeilan RI, Alcaro S, Croce CM and Trapasso F. Fhit delocalizes annexin a4 from plasma membrane to cytosol and sensitizes lung cancer cells to Paclitaxel. PLoS One. 2013; 8(11):e78610

Biochemical and Biophysical Research Communications 456 (2015) 908–912

Contents lists available at ScienceDirect

Biochemical and Biophysical Research Communications

journal homepage: www.elsevier.com/locate/ybbrc

Generation and characterization of a bispecific diabody targeting both EPH receptor A10 and CD3

Haruhiko Kamada [a,b,1], Shintaro Taki [a,c,1], Kazuya Nagano [a], Masaki Inoue [a], Daisuke Ando [a,c], Yohei Mukai [a,d], Kazuma Higashisaka [a,e], Yasuo Yoshioka [a,b,e], Yasuo Tsutsumi [a,b,d,e], Shin-ichi Tsunoda [a,b,c,d,*]

[a] Laboratory of Biopharmaceutical Research, National Institute of Biomedical Innovation, 7-6-8 Saito-Asagi, Ibaraki, Osaka 567-0085, Japan
[b] The Center for Advanced Medical Engineering and Informatics, Osaka University, 1-6 Yamadaoka, Suita, Osaka 565-0871, Japan
[c] Laboratory of Biomedical Innovation, Graduate School of Pharmaceutical Sciences, Osaka University, 1-6 Yamadaoka, Suita, Osaka 565-0871, Japan
[d] Laboratory of Innovative Antibody Engineering and Design (iAED), Center for Drug Innovation and Screening, National Institute of Biomedical Innovation, 7-6-8 Saito-Asagi, Ibaraki, Osaka 567-0085, Japan
[e] Laboratory of Toxicology and Safety Science, Graduate School of Pharmaceutical Sciences, Osaka University, 1-6 Yamadaoka, Suita, Osaka 565-0871, Japan

ARTICLE INFO

Article history:
Received 26 November 2014
Available online 17 December 2014

Keywords:
Bispecific antibody
Diabody
EPHA10
CD3
Redirected T cell response

ABSTRACT

The EPH receptor A10 (EphA10) is up-regulated in breast cancer but is not normally expressed in healthy tissue, thus it has been suggested that EphA10 may be a useful target for cancer therapy. This study reports a diabody, an antibody derivative binding two different target molecules, EphA10 expressed in tumor cells and CD3 expressed in T cells, which showed T cell dependent-cytotoxicity. The diabody, which has His-tagged and FLAG-tagged chains, was expressed in *Escherichia coli* and purified in both heterodimer (Db-1) and homodimer (Db-2) formulations by liquid chromatography. Flow cytometry analysis using EphA10-expressing cells showed that binding activity of heterodimers was stronger than that of homodimers. Addition of diabodies to PBMC cultures resulted in T-cell mediated redirected lysis, and the bioactivity was consistent with the stronger binding activity of heterodimeric diabody formulations. Our results indicate that diabodies recognizing both EphA10 and CD3 could have a range of potential applications in cancer therapy, such as breast cancers that express the EPH receptor A10, especially triple negative breast cancer.

1. Introduction

The EPH receptor A10 (EphA10) [1], known as an ephrin receptor family protein, is known to be involved in cancer progression. The roles of EphA10 in cancer have not yet been fully elucidated [2], although it has been shown to be a contributing factor in tumor progression and invasion and has been associated with enhanced tumorigenic properties and reduced survival times in breast carcinoma. Its expression in normal human tissue seems to be confined to the testis [1] and it is up-regulated in several cancers including prostate cancer [3], ovarian cancer and breast cancer [4,5]. EphA10 transcripts are absent in normal prostate and breast cells but are present in cancer cells of prostate and breast, respectively. Interestingly, high levels of EphA10 are found in the context of triple negative breast cancers (TNBCs) [5]. Targeting EphA10 by blocking EphA10-dependent activation of the MAPK pathway has resulted in tumor growth inhibition *in vivo*. Therefore, EphA10 has emerged as a promising target for antibody therapies, while the exact functions and mechanism of action of EphA10 in normal physiology or in pathological conditions remain to be determined.

Creating bispecific antibodies (BsAbs), which are capable of simultaneous binding to two different targets, could overcome many defects of monoclonal antibody therapies [6]. Such molecules would be able to retarget not only a large variety of cancer cells but other cell types as well, such as lymphocytes [7–9]. The potential of this approach has been demonstrated by several studies and large amounts of heterogeneous BsAbs have been produced using techniques of molecular biology. In particular, a diabody, which is a kind of BsAb, is constructed from non-covalently associated bivalent molecules, created from scFvs by shortening the polypeptide linker between the VH and VL domains [10–13]. These antibody derivatives may be used as therapeutic drugs to treat cancer and blood coagulation diseases.

* Corresponding author at: Laboratory of Biopharmaceutical Research, National Institute of Biomedical Innovation, 7-6-8 Saito-Asagi, Ibaraki, Osaka 567-0085, Japan. Fax: +81 72 641 9817.
E-mail address: tsunoda@nibio.go.jp (S.-i. Tsunoda).
[1] These authors contributed equally to the work.

http://dx.doi.org/10.1016/j.bbrc.2014.12.030
0006-291X/

Antibodies that react specifically with EphA10 could have diagnostic and therapeutic utility, particularly if they show functional blocking activity. Towards this end, we previously created murine IgG reactive with EphA10 [5]. This anti-EphA10 antibody, in full IgG format, showed anti-tumor activity against breast cancer model mice, however, the effect of BsAb against EphA10-expressing cells was not clear. Here we describe the development of an anti-EphA10 and CD3 BsAb in diabody format. The bivalent nature of diabodies is advantageous for targeting and they provide a flexible platform for development of targeted therapeutics. The anti-EphA10 and CD3 diabody showed cytotoxicity *in vitro* against EphA10-expressing cells.

2. Materials and methods

2.1. Cell lines and culture

Hybridoma 38.1 (mouse Hybridoma HB-231) and MDA-MB-435 (human breast cancer cell line HTB-129) cells were obtained from American Type Culture Collection (ATCC, Rockville, MD) and cultured under the recommended conditions. Human cells that overexpressed EphA10, MDA-MB-435 (MDA-MB-435^{EphA10}), were established in our laboratory. In brief, a lentiviral vector encoding human EphA10 was transfected into MDA-MB-435 cells and stably transfected cells were obtained by Blasticidin (Invitrogen) selection. A hybridoma producing anti-EphA10 IgG was established from splenocytes of a human EphA10-immunized mouse by fusion with a mouse myeloma line.

2.2. Cloning of variable (V) immunoglobulin domains

The genes of V light-chain (VL) and V heavy-chain (VH) domains from each hybridoma were subcloned using 5′-Full RACE kits (Takara Bio, Kyoto, Japan). The amplified DNA was directionally subcloned into a plasmid vector using the TOPO TA cloning kit (Invitrogen) and sequenced using a 3130xl Genetic Analyzer (Applied Biosystems, Carlsbad, CA).

2.3. Vector construction

The vectors to express the bispecific antibody or single chain Fv (scFv), respectively, were constructed as described previously [14]. The primer sequences are shown in Table 1. To construct the co-expression vector, two additional restriction sites (*Sac*II, *Spe*I) were inserted into the pET20b vector (Invitrogen) and the new vector was named pET20b (SS+). The *E. coli* TOP10 strain (Invitrogen) was used to subclone target genes. To obtain a scFv A (EphA10-VL-Linker-CD3-VH) and a scFv B (CD3-VL-Linker-EphA10-VH), the corresponding VL and VH regions were cloned into separate vectors as templates for VL- and VH-specific PCR using the primer pairs 5′ *Nco*I-VL (hEphA10 or hCD3)/3′ VL (hEphA10 or hCD3)-Linker and 5′ Linker-VH (hEphA10 and hCD3)/3′ VH (hCD3)-*Not*I (scFv A) or 3′ VH (hEphA10)-FLAG tag (DYKDDDDKA) *Xho*I (scFv B), respectively. Overlapping complementary sequences were introduced into the PCR products, which combined to form the coding sequence of the 5-amino acid (G_4S) Linker during the subsequent fusion PCR. This amplification step was performed with the primer pair 5′ *Nco*I-VL (hEphA10 or hCD3)/3′ VH (hCD3)-*Not*I (scFv A) or 3′ VH (hEphA10)-FLAG tag *Xho*I (scFv B), and the resulting fusion product was cleaved with the restriction enzymes *Nco*I and *Not*I (scFv A) or *Xho*I (scFv B), then cloned into the pET20b (SS+) vector (scFv A) and pET20b vector (scFv B). Next, to construct the bispecific antibody (diabody) expression vector, the previously described scFv B vector was used as a template for scFv-specific PCR with the primer pair 5′ *Sac*II-pelB/3′ FLAG-tag-stop-*Spe*I. The PCR product was cleaved with the restriction enzymes *Sac*II and *Spe*I, then cloned into the pET20b (SS+) scFv A vector (pET20b (SS+) diabody).

2.4. Expression and purification of the diabody

In order to express the bispecific diabody, plasmid pET20b (SS+) diabody was transformed into *E. coli* BL21 (DE3) Star (Invitrogen). *Escherichia coli* cells containing the recombinant plasmids were inoculated into 3 ml of 2xYT medium containing 1 mg/ml ampicillin. Overnight cultures were transferred to 300 ml of fresh medium and were grown at 37 °C until they reached an A_{600} = 0.8. Isopropyl-β-D-thiogalactopyranoside (IPTG) was added to a final concentration of 0.5 mM and the cultures were further grown overnight at 20 °C. *E. coli* cells were collected by centrifugation (8000*g* for 20 min at 4 °C) and re-suspended in Osmotic Shock buffer (20 mM Tris–HCl, pH 8.0, 0.5 M sucrose, and EDTA added to 0.1 mM final). After 1 h incubation at 4 °C, the cells were shocked by adding ice water and then centrifuged (8000*g* for 30 min at 4 °C). The diabody-containing supernatant was brought to 60% ammonium sulfate and stirred gently overnight. The diabody was precipitated by centrifugation (8000*g* for 30 min at 4 °C). The protein pellet was resuspended in phosphate-buffered saline (PBS) buffer and dialysed exhaustively against PBS at 4 °C.

After dialysis, the diabody was purified by immobilized metal affinity chromatography (IMAC). The diabody was eluted using 150 mM imidazole/PBS (Db-1 Elution) and 300 mM imidazole/PBS (Db-2 Elution) buffers. Each fraction was subjected to gel filtration chromatography with a Superdex200 prep grade column (GE Healthcare, Little Chalfont Bucks, UK) equilibrated in PBS. SDS–PAGE and Western blot analysis with an anti-His or anti-FLAG tag antibody were performed to detect and confirm the size and purity of the diabody-containing fractions. Purified proteins were concentrated in PBS by ultrafiltration with a Centriprep® 30 K or 50 K

Table 1
Oligonucleotide sequences of PCR primers used for construction of diabody (EphA10/CD3) vector.

Primer	Nucleotide sequence (5′–3′)[a]
5′ NcoI-VL (hEphA10)	NNNCCATGGCCAGTTTTGTGATGACCCAGACTCCC
3′ VL (hEphA10)-Linker	CTGGCTACCACCACCACCAGCCCGTTTGATTTCCAGCTTGGT
5′ Linker-VH (hEphA10)	GAAAGGTGGTGGTGGTAGCCAGGTTCTGCTGCAGCAGTCT
3′ VH (hEphA10)-FLAG-*Xho*I	NNNCTCGAGTCATCAGGCCTTGTCATCGTCATCCTTGTAGTCTGAGGAGACGGTGACTGAGGTT
5′ *Nco*I-VL (hCD3)	NNNCCATGGCCCAAATTGTTCTCACCCAGTCTCCAG
3′ VL (hCD3)-Linker	CTGGCTACCACCACCACCTTTCAGCTCCAGCTTGGTCCC
5′ Linker-VH (hCD3))	GCTGGTGGTGGTGGTAGCCAGGTCCAGCTGCAGCAGT
3′ VH (hCD3)-*Not*I	NNNGCGGCCGCTGAGGAGACGGTGACTGAGGTT
5′ *Sac*II-pelB	NNNCCGCGGATGAAATACCTGCTGCCGACCG
3′ FLAG-tag-stop-*Spe*I	NNNACTAGTTCATCAGGCCTTGTCATCGTCATC

[a] The restriction enzyme site is underlined.

device (Millipore, Billerica, MA, USA), and protein concentrations were estimated using a Coomassie Plus Protein Assay kit (Thermo Fisher Scientific, Rockford, IL).

2.5. Flow cytometric analysis

MDA-MB-435 or MDA-MB-435^{EphA10} (5×10^5 cells) were suspended in Suspension buffer (2% FBS containing PBS) and incubated with 20 μg diabody or 2 μg control IgG (anti-EphA10, anti-CD3) for 1 h on ice, respectively. After washing with Suspension buffer, the cells were incubated with Surelight P3 (614 nm excitation and 662 nm emission) labeled antibodies against the His tag (Columbia Biosciences, Frederick, MD) and Surelight P3 labeled antibodies against the mouse IgG (Columbia Biosciences) for 1 h on ice. The cells were washed again and resuspended in 500 μL Suspension buffer and flow cytometric analysis was performed (FACScanto; BD Biosciences, San Jose, CA). All tests were carried out in triplicate.

2.6. Cytotoxicity assays

Cytotoxicity assays were performed as described previously with slight modifications [14]. In brief, MDA-MB-435^{EphA10} cells and MDA-MB-435 parent cells as target cells (10^3 cells/well) were added to 96-well plates with 10% FBS containing D-MEM at 37 °C in a humidified atmosphere containing 5% CO_2. After overnight culture, supernatants were removed and non-stimulated human PBMC from healthy donors as effector cells were added to an effector-to-target (E/T) ratio of 10 with each of the antibodies (0.1–10 μg/mL), respectively. After 48 h of incubation, lactate dehydrogenase (LDH) released into the supernatant was measured using a CytoTox 96® non-radioactive cytotoxicity assay (Promega, Madison, WI). Percentages of specific lysis were calculated according to the formula: % cytotoxicity = [(experimental release) − (effector spontaneous release) − (target spontaneous release)]/[(target maximum release) − (target spontaneous release)] × 100. All tests were carried out in triplicate.

2.7. Statistical analysis

Differences in cytotoxicity assay results between the control and target groups were compared using the unpaired Student's *t*-test.

3. Result and discussion

3.1. Formulations of diabody binding to EphA10 and CD3

A BsAb was constructed using two different scFv fragments (scFv A and scFv B) derived from the anti-EphA10 IgG and anti-CD3 IgG. His-tagged and FLAG-tagged VL-VH chain (EphA10-VL-Linker-CD3-VH; scFv A and CD3-VL-Linker- EphA10-VH; scFv

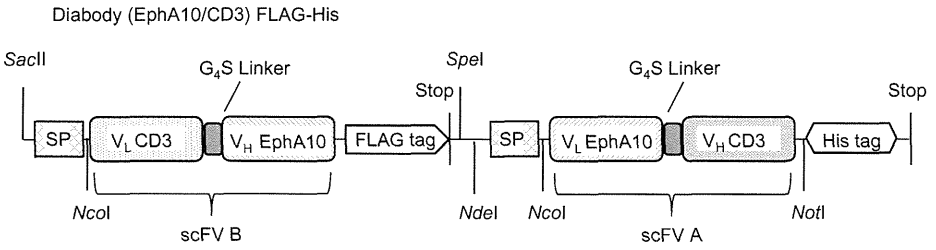

Fig. 1. Construction of the diabody-expressing vector.

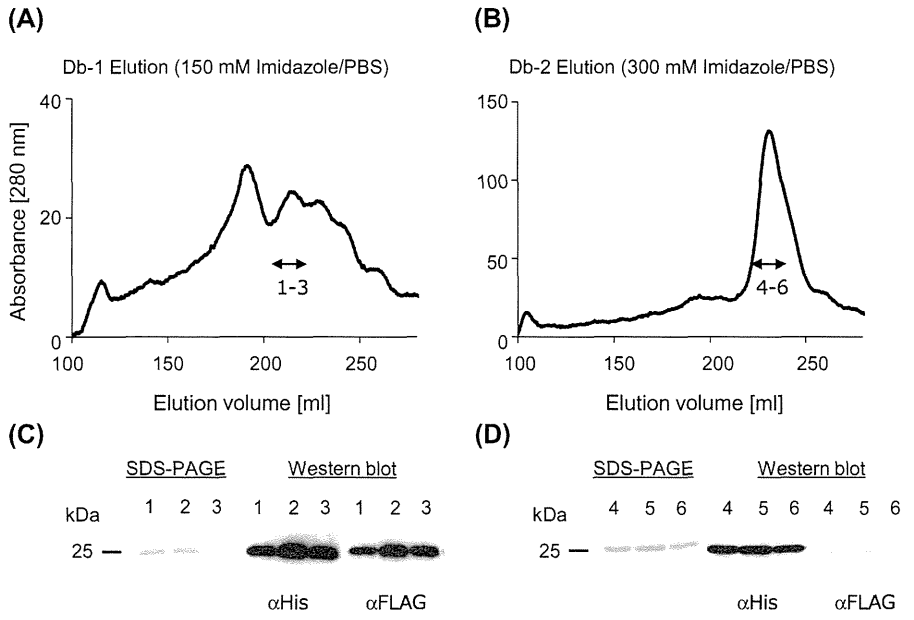

Fig. 2. Characteristics of diabody (Db-1 and Db-2). Gel filtration chromatography profile of diabodies, which were purified by IMAC. (A) 150 mM imidazole elution pattern (Db-1 as heterodimer) and (B) 300 mM imidazole elution pattern (Db-2 as homodimer). SDS–PAGE and Western blot analysis of dimeric Db-1 (C) and Db-2 (D). The line indicates the apparent molecular weight (25 kDa).

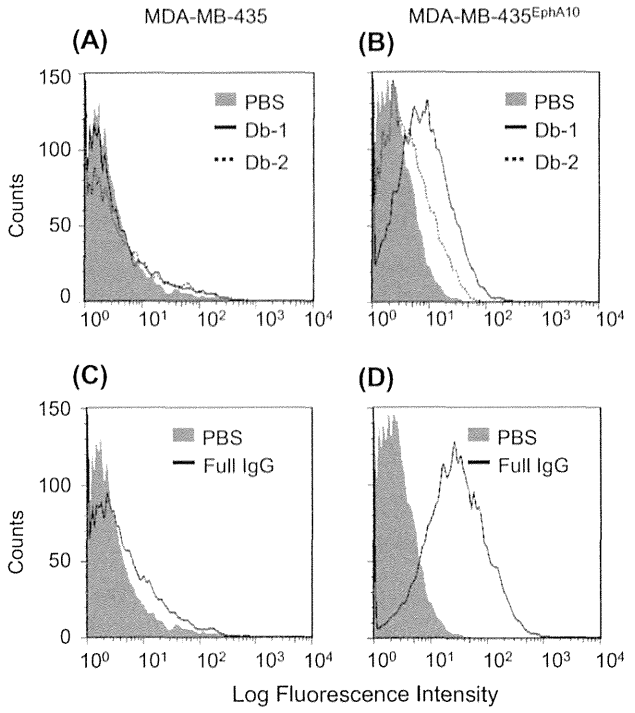

Fig. 3. Binding activity of diabody against EphA10-transfected cells and the parent cells (MDA-MD-435). The left panels (A, C) show the binding ability of the diabodies (A) and of the full IgG (C) against parental cells (MDA-MB-435) and the right panels (B, D) are against EphA10-transfeted cells. Binding activities were measured using 20 μg of each diabody sample. Cell-binding proteins were detected using SureLight P3 conjugated anti-His tag or anti-mouse IgG mAb. Filled bars are vehicle control (PBS).

B, respectively) were constructed (Fig. 1). The plasmid vector construct was designed by adding an N-terminal signal peptide to express BsAb in a soluble form and adding a C-terminal hexahistidine (His × 6) tag or FLAG tag to allow purification by affinity chromatography on a Ni-Sepharose column. This plasmid vector was transfected into BL21 (DE3) Star *E. coli* cells. Pooled supernatants were purified by IMAC using two elution buffers, and fractions containing the diabody further purified by gel-filtration chromatography (Fig. 2A and B). SDS–PAGE under reducing conditions followed by Western blot analysis showed only a single band indicating a ~25 kDa protein (Fig. 2C and D), consistent with the calculated molecular mass of approximately 25 kDa for each scFv. Because these two scFv chains are structured as homodimers, they would be expected to show only low binding activity compared with the heterodimeric form that can fully recognize the target molecules. Therefore, the diabody formulation was checked by western blot against both an anti-His and an anti-FLAG antibody (Fig. 2C and D). These results showed that the diabody existed as heterodimer in the condition of 150 mM imidazole elution, because the amounts of His- and FLAG-tagged scFvs were similar (Fig. 2C). However, the fraction eluted by 300 mM imidazole was primarily composed of homodimers, because the anti-His-tag staining was much stronger than the anti-FLAG tag staining (Fig. 2D). Because His-tagged homodimer antibodies would get trapped strongly by a Ni-Sepharose column, two concentrations of imidazole were used to elute the scFvs (Db-1: 150 mM imidazole/PBS, Db-2: 300 mM imidazole/PBS). The heterodimers indeed were eluted at a lower imidazole concentration than the homodimers.

3.2. Binding activity of diabody for human EphA10

Binding activities of these diabodies (Db-1 and Db-2) were examined by flow cytometric analysis using the MDA-MB-435 parental cells, MDA-MB-435^{EphA10} cells. Specific binding of EphA10 antigens to both Db-1 and Db-2 was observed (Fig. 3). Interestingly, the binding activity of diabody Db-1 was stronger than that of Db-2. These results indicated that the binding activity of the homodimer was reduced because this formulation would have mismatches between each VL and VH. Furthermore, the structural difference between homodimers and heterodimers had a significant effect on the binding activity.

3.3. Redirected target cell lysis of diabody with PBMC

The efficacy of T-cell mediated redirected lysis of MDA-MB-435^{EphA10} cells and the parental cells following addition of each diabody was examined using an LDH cytotoxicity assay. Non-stimulated PBMC were used as effector cells at E/T ratios of 10, respectively. As shown in Fig. 4, the Db-1 and Db-2 diabodies showed dose-dependent cytotoxic activity against MDA-MB-435^{EphA10} cells compared with the scFv constructs (anti-EphA10 scFV). Furthermore, the cytotoxic efficacy of Db-1 was higher than that of Db-2 at low antibody concentrations, indicating that the heterodimer would increase the cytotoxicity related to binding of the antigen.

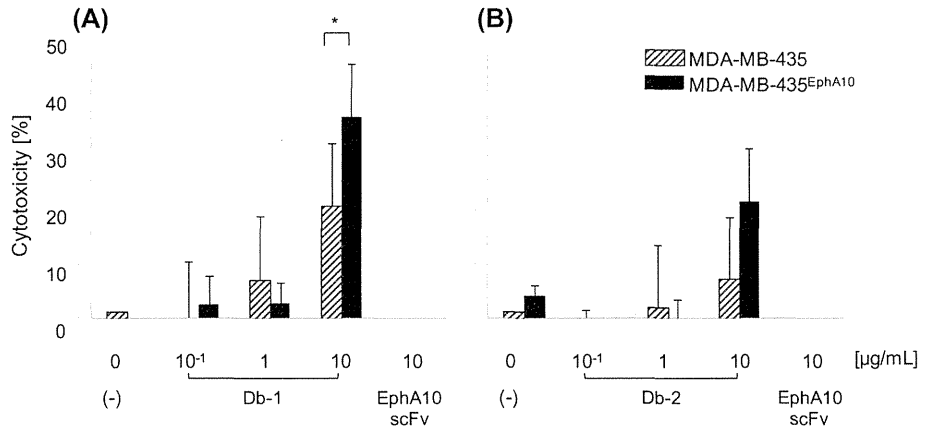

Fig. 4. *In vitro* cytotoxicity of diabody formulations (Db-1 and Db-2) against MDA-MB-435^{EphA10} and parental cells. The left panels are heterodimeric diabody, Db-1 (A) and the right panels are homodimeric diabody, Db-2 (B). MDA-MB-435 parental cells (slashed column) and MDA-MB-435^{EphA10} (black column) cells were co-cultured respectively with human PBMC at E/T ratios of 10. Each point represents the mean of triplicate determinations; error bars represent the standard deviations of triplicate determinations. Asterisks label readings that were statistically significant (unpaired Student's *t*-test) from MDA-MB-435 and MDA-MB-435^{EphA10} ($^*P \leq 0.05$).

The results of this study demonstrate that heterodimeric diabodies can show potent binding activity and specificity against cells that express the target antigen. Purified heterodimeric diabody formulations would lead to higher activity because of their increased affinity against two antigens, compared to homodimers or mixtures of homodimers plus heterodimers. Therefore, it is necessary to optimize purification protocols using HPLC etc. However, diabody formulations consisting of two chains of VL and VH could in principle form several types of mixed species. Thus, the protocols for bispecific antibodies should be optimized to produce a formulation containing a single species, e.g. by using linkers to produce a single chain diabody or tandem scFV. This should improve and standardize the desired binding functions of the BsAbs. The construction of such modified antibodies, e.g. scDb and faFV, shows great potential for the development of novel therapeutic drugs.

Acknowledgment

This work was supported by JSPS KAKENHI Grant Number 24680093.

References

[1] H.C. Aasheim, S. Patzke, H.S. Hjorthaug, E.F. Finne, Characterization of a novel Eph receptor tyrosine kinase, EphA10, expressed in testis, Biochim. Biophys. Acta 1723 (2005) 1–7.
[2] L. Truitt, A. Freywald, Dancing with the dead: Eph receptors and their kinase-null partners, Biochem. Cell Biol. 89 (2011) 115–129.
[3] K. Nagano, T. Yamashita, M. Inoue, K. Higashisaka, Y. Yoshioka, Y. Abe, Y. Mukai, H. Kamada, Y. Tsutsumi, S. Tsunoda, Eph receptor A10 has a potential as a target for a prostate cancer therapy, Biochem. Biophys. Res. Commun. 450 (2014) 545–549.
[4] K. Nagano, S. Kanasaki, T. Yamashita, Y. Maeda, M. Inoue, K. Higashisaka, Y. Yoshioka, Y. Abe, Y. Mukai, H. Kamada, Y. Tsutsumi, S. Tsunoda, Expression of Eph receptor A10 is correlated with lymph node metastasis and stage progression in breast cancer patients, Cancer Med. 2 (2013) 972–977.
[5] K. Nagano, Y. Maeda, S. Kanasaki, T. Watanabe, T. Yamashita, M. Inoue, K. Higashisaka, Y. Yoshioka, Y. Abe, Y. Mukai, H. Kamada, Y. Tsutsumi, S. Tsunoda, Ephrin receptor A10 is a promising drug target potentially useful for breast cancers including triple negative breast cancers, J. Control. Release 189 (2014) 72–79.
[6] D. Schrama, R.A. Reisfeld, J.C. Becker, Antibody targeted drugs as cancer therapeutics, Nat. Rev. Drug Discovery 5 (2006) 147–159.
[7] M.K. Gleason, J.A. Ross, E.D. Warlick, T.C. Lund, M.R. Verneris, A. Wiernik, S. Spellman, M.D. Haagenson, A.J. Lenvik, M.R. Litzow, P.K. Epling-Burnette, B.R. Blazar, L.M. Weiner, D.J. Weisdorf, D.A. Vallera, J.S. Miller, CD16xCD33 bispecific killer cell engager (BiKE) activates NK cells against primary MDS and MDSC CD33+ targets, Blood 123 (2014) 3016–3026.
[8] C. Somasundaram, R. Arch, S. Matzku, M. Zoller, Development of a bispecific F(ab')2 conjugate against the complement receptor CR3 of macrophages and a variant CD44 antigen of rat pancreatic adenocarcinoma for redirecting macrophage-mediated tumor cytotoxicity, Cancer Immunol. Immunother. 42 (1996) 343–350.
[9] S.R. Frankel, P.A. Baeuerle, Targeting T cells to tumor cells using bispecific antibodies, Curr. Opin. Chem. Biol. 17 (2013) 385–392.
[10] I. Shimomura, S. Konno, A. Ito, Y. Masakari, R. Orimo, S. Taki, K. Arai, H. Ogata, M. Okada, S. Furumoto, M. Onitsuka, T. Omasa, H. Hayashi, Y. Katayose, M. Unno, T. Kudo, M. Umetsu, I. Kumagai, R. Asano, Rearranging the domain order of a diabody-based IgG-like bispecific antibody enhances its antitumor activity and improves its degradation resistance and pharmacokinetics, MAbs 6 (2014).
[11] R. Asano, T. Kumagai, K. Nagai, S. Taki, I. Shimomura, K. Arai, H. Ogata, M. Okada, F. Hayasaka, H. Sanada, T. Nakanishi, T. Karvonen, H. Hayashi, Y. Katayose, M. Unno, T. Kudo, M. Umetsu, I. Kumagai, Domain order of a bispecific diabody dramatically enhances its antitumor activity beyond structural format conversion: the case of the hEx3 diabody, Protein Eng. Des. Sel. 26 (2013) 359–367.
[12] R. Asano, K. Ikoma, I. Shimomura, S. Taki, T. Nakanishi, M. Umetsu, I. Kumagai, Cytotoxic enhancement of a bispecific diabody by format conversion to tandem single-chain variable fragment (taFv): the case of the hEx3 diabody, J. Biol. Chem. 286 (2011) 1812–1818.
[13] R. Asano, K. Ikoma, Y. Sone, H. Kawaguchi, S. Taki, H. Hayashi, T. Nakanishi, M. Umetsu, Y. Katayose, M. Unno, T. Kudo, I. Kumagai, Highly enhanced cytotoxicity of a dimeric bispecific diabody, the hEx3 tetrabody, J. Biol. Chem. 285 (2010) 20844–20849.
[14] A. Loffler, P. Kufer, R. Lutterbuse, F. Zettl, P.T. Daniel, J.M. Schwenkenbecher, G. Riethmuller, B. Dorken, R.C. Bargou, A recombinant bispecific single-chain antibody, CD19 × CD3, induces rapid and high lymphoma-directed cytotoxicity by unstimulated T lymphocytes, Blood 95 (2000) 2098–2103.

Biochemical and Biophysical Research Communications 450 (2014) 545–549

Contents lists available at ScienceDirect

Biochemical and Biophysical Research Communications

journal homepage: www.elsevier.com/locate/ybbrc

Eph receptor A10 has a potential as a target for a prostate cancer therapy

Kazuya Nagano [a], Takuya Yamashita [a,b], Masaki Inoue [a], Kazuma Higashisaka [a,b], Yasuo Yoshioka [a,b,c], Yasuhiro Abe [d], Yohei Mukai [e], Haruhiko Kamada [a,c], Yasuo Tsutsumi [b,c,e], Shin-ichi Tsunoda [a,b,c,e,*]

[a] Laboratory of Biopharmaceutical Research, National Institute of Biomedical Innovation, 7-6-8 Saito-Asagi, Ibaraki, Osaka 567-0085, Japan
[b] Graduate School of Pharmaceutical Sciences, Osaka University, 1-6 Yamadaoka, Suita, Osaka 565-0871, Japan
[c] The Center of Advanced Medical Engineering and Informatics, Osaka University, 1-6 Yamadaoka, Suita, Osaka 565-0871, Japan
[d] Cancer Biology Research Center, Sanford Research/USD, 2301 E. 60th Street N, Sioux Falls, SD 57104, USA
[e] Laboratory of Innovative Antibody Engineering and Design, National Institute of Biomedical Innovation, 7-6-8 Saito-Asagi, Ibaraki, Osaka 567-0085, Japan

ARTICLE INFO

Article history:
Received 28 May 2014
Available online 9 June 2014

Keywords:
Eph receptor A10
Prostate cancer
Antibody drug

ABSTRACT

We recently identified Eph receptor A10 (EphA10) as a novel breast cancer-specific protein. Moreover, we also showed that an in-house developed anti-EphA10 monoclonal antibody (mAb) significantly inhibited proliferation of breast cancer cells, suggesting EphA10 as a promising target for breast cancer therapy. However, the only other known report for EphA10 was its expression in the testis at the mRNA level. Therefore, the potency of EphA10 as a drug target against cancers other than the breast is not known. The expression of EphA10 in a wide variety of cancer cells was studied and the potential of EphA10 as a drug target was evaluated. Screening of EphA10 mRNA expression showed that EphA10 was overexpressed in breast cancer cell lines as well as in prostate and colon cancer cell lines. Thus, we focused on prostate cancers in which EphA10 expression was equivalent to that in breast cancers. As a result, EphA10 expression was clearly shown in clinical prostate tumor tissues as well as in cell lines at the mRNA and protein levels. In order to evaluate the potential of EphA10 as a drug target, we analyzed complement-dependent cytotoxicity effects of anti-EphA10 mAb and found that significant cytotoxicity was mediated by the expression of EphA10. Therefore, the idea was conceived that the overexpression of EphA10 in prostate cancers might have a potential as a target for prostate cancer therapy, and formed the basis for the studies reported here.

1. Introduction

The development of antibody engineering has enabled a monoclonal antibody (mAb) to become a safe and effective drug for refractory diseases, such as cancer. Today, more than 30 kinds of antibody drugs are approved all over the world. Continued growth in the market is expected in the future [1]. However, the cases to which antibody drugs are applied are limited. Therefore, the development of new antibody drugs is especially needed in the cases without effective treatments, such as a triple negative breast cancer, a castration-resistant prostate cancer, as well as pancreatic cancers or malignant mesotheliomas.

Several Eph receptor family members such as EphA2 or EphB4 are highly expressed in various tumor cell types found in refractory cancers [2], and with expressions associated with tumorigenesis [3,4], proliferation [5,6], vasculogenesis [7,8] and metastasis [9,10]. Therefore, there is a current focus on the development of therapies targeted on Eph members [11]. In this context, MedImmune LLC is developing an antibody-drug conjugate against EphA2 which inhibits tumor growth *in vitro* and *in vivo* [12,13]. It has been tested in phase I to investigate the safety profile and maximum tolerated dose. However, the most recent report announced the trial was stopped halfway due to adverse events such as bleeding and liver disorders [14]. Some databases such as MOPED or PaxDb have reported that EphA2 is highly expressed in platelets and liver tissues. Therefore, the target protein needs to display specific expression in cancer tissues. However, EphA10 which we identified as a novel breast cancer-related protein is hardly expressed in normal human tissues [15] [16]. Furthermore, we also showed that an in-house developed anti-EphA10 mAb inhibited breast cancer cell proliferation at both *in vitro* and *in vivo* levels [16]. These findings

Abbreviations: EphA10, Eph receptor A10; mAb, monoclonal antibody; TMA, tissue microarray; HMEC, human mammary epithelial cell; PrEC, prostate epithelial cell; cDNA, complimentary DNA; FCS, fetal calf serum; PBS, phosphate buffered saline; IHC, immunohistochemistry; CDC, complement-dependent cytotoxicity.

* Corresponding author. Fax: +81 72 641 9817.
E-mail address: tsunoda@nibio.go.jp (S.-i. Tsunoda).

http://dx.doi.org/10.1016/j.bbrc.2014.06.007
0006-291X/

suggest that EphA10 is a promising target for breast cancer therapy. However, the only other known report was that EphA10 is expressed in the testis at the mRNA level [17]. Therefore, the potency of EphA10 as a drug target against cancers other than the breast has not been tested. Here, we report EphA10 expression in various kinds of cancer cells and the potential of EphA10 as a target in other cancer therapies.

2. Material and methods

2.1. Cell lines

The following cancer cell lines were purchased from the American Type Culture Collection (Manassas, VA): HCC70, MDA-MB-157, HCC1599, MDA-MB468, DU4475, 22Rv1, VCaP, colo201, SW620, HCT116, BxPC3, Panc1, AsPC1, H2452, H2052, H28 and Jurkat. The following cancer cell lines were purchased from the Japanese Collection of Research Bioresources Cell Bank (Osaka, Japan): RERF-LC-KJ, RERF-LC-MS, MKN1, MKN45, NEC8, NEC14, A2058, G318, Mewo and K562. PC3 and LNCaP were purchased from the Riken Bioresource Center Cell Bank (Ibaraki, Japan). Normal Human Prostate Epithelial Cells (PrEC) and Normal Human Mammary Epithelial Cells were purchased from Lonza (Basel, Switzerland). All cells were cultured at 37 °C in a humidified atmosphere of 5% CO_2 according to the provider's protocol.

2.2. Real-time PCR

Complementary DNAs (cDNAs) derived from human prostate tumors were purchased from OriGene Technologies (Rockville, MD). The PCR mixture included cDNA template, TaqMan Gene Expression Master Mix and TaqMan probe (EphA10: Hs01017018_m1 or actin-beta: Hs99999903_m1) (Life Technologies, Carlsbad, CA) and the reaction was performed according to the manufacturer's instructions. The threshold cycles were determined using the default settings. EphA10 mRNA expression levels were normalized against actin-beta.

2.3. Cell immunofluorescent staining

PrEC, PC3 and VCaP cells were seeded at 1×10^4 cells/well in Lab-Tek™ 8-well chamber slides (Thermo Fisher Scientific Inc., Waltham, MA). After 24 h, cells were washed twice with PBS, and then fixed with PBS containing 4% paraformaldehyde, pH 8.0 for 10 min. After washing with PBS, fixation was quenched with PBS containing 0.1 M glycine, pH 7.4 for 15 min. Fixed cells were blocked with PBS containing 5% FCS (blocking solution), pH 7.4 for 30 min, and then treated with the anti-EphA10 monoclonal primary antibody and isotype control antibody at 10 μg/ml in blocking solution for 1 h. Donkey anti-mouse IgG conjugated with Alexa Flour 488 (Life Technologies, Carlsbad, CA) was used as the second antibody at 2 μg/ml in the blocking solution for 1 h in the dark. Slides were mounted using a vectashield mounting medium for fluorescence with DAPI (Vector Laboratories Inc., Burlingame, CA) and analyzed with a Leica TCS SP2 confocal laser scanning microscope (Leica Microsystems GmbH, Wetzlar, Germany). Images were further processed using the Adobe Photoshop software.

2.4. Immunohistochemical (IHC) staining

TMAs with prostate tumor and normal prostate tissues (US Biomax, Rockville, MD) were deparaffinized in xylene and rehydrated in a graded series of ethanol. Heat-induced epitope retrieval was performed by maintaining the Target Retrieval Solution (Dako, Glostup, Denmark) by following the manufacturer's instructions. After treatment, endogenous peroxidase was blocked with 0.3%. The TMA slides were incubated with rabbit anti-human EphA10 polyclonal antibody (Abgent Inc., San Diego, CA) for 30 min and then with ENVISION+ Dual Link (Dako, Glostup, Denmark) for 30 min. The reaction products were rinsed three times with 0.05% Tween20/Tris buffer saline and then developed in liquid 3,3′-diaminobenzidine for 3 min. After development, sections were lightly counterstained with Mayer's hematoxylin. All procedures were performed using an AutoStainer (Dako, Glostup, Denmark). Study samples were divided into high and low expression groups based on the two criteria of distribution and quantity. In terms of distribution, the percentage of positive cells across all tumor cells

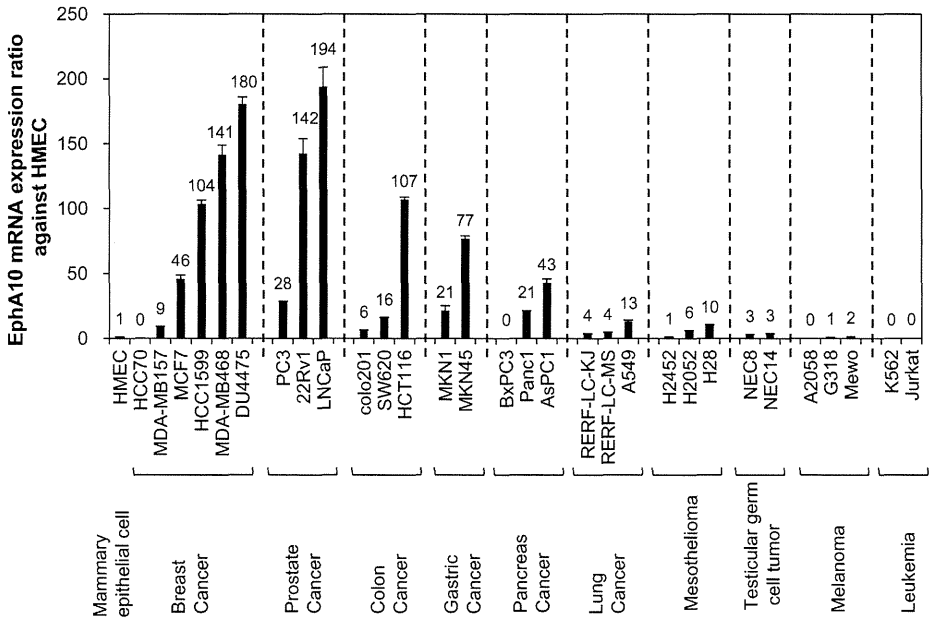

Fig. 1. Screening of EphA10 expression profile in various kinds of cancer cell lines. EphA10 expression in various kinds of cancer cells were screened by quantitative real time PCR. EphA10 expression level in each cell was normalized by actin-beta expression level and described as a ratio against EphA10 expression level in HMEC, normal human mammary epithelial primary cells. $n = 3$ in each group. Error bars represent the SD.

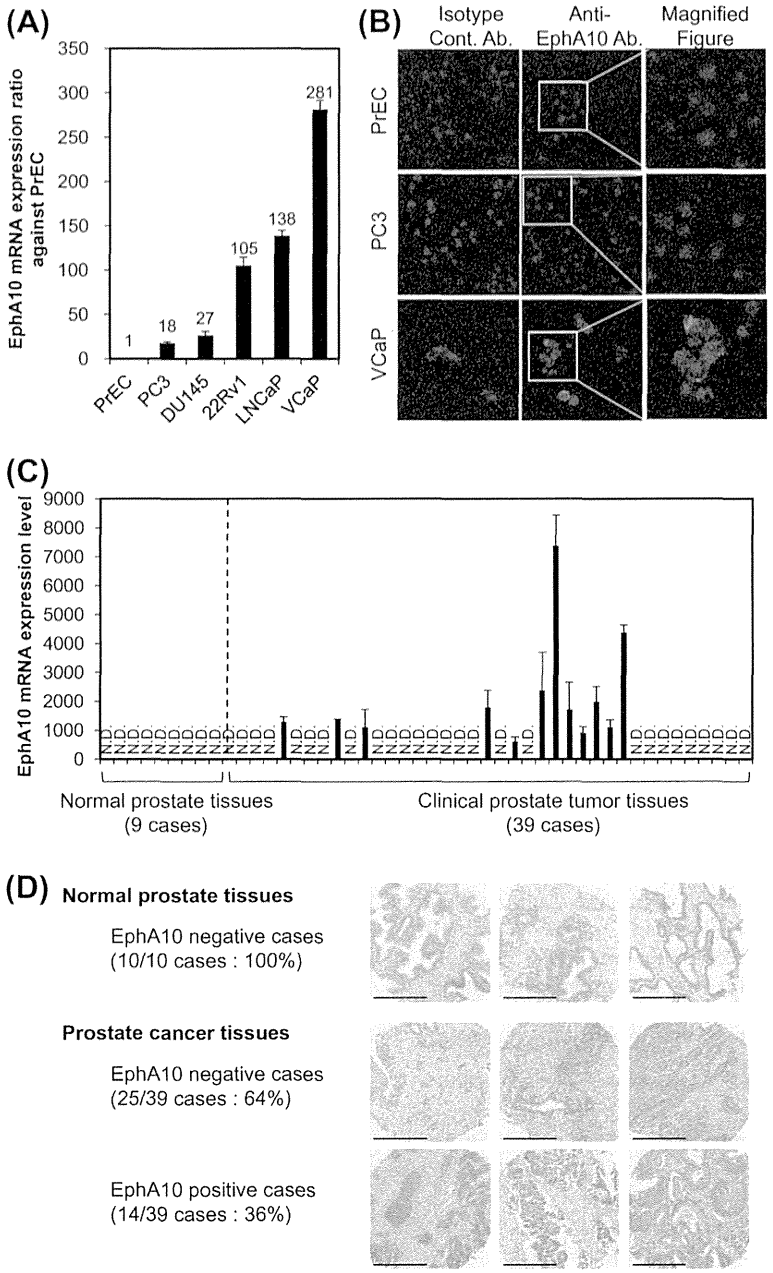

Fig. 2. EphA10 expression analysis in prostate cancer cell lines and clinical prostate cancer tissues at mRNA and protein level. (A) EphA10 mRNA expression level in prostate cancer cell lines (PC3, DU145, 22Rv1, LNCaP and VCaP) was quantified by real time PCR. It was normalized by actin-beta expression level and described as a ratio against EphA10 expression level in PrEC, normal human prostate epithelial primary cells. $n = 3$ in each group. Error bars represent the SD. (B) EphA10 protein expression in prostate cancer cell lines was analyzed by cell immunofluorescent staining. PrEC, PC3 (EphA10-mRNA low expressing cells) and VCaP (EphA10 mRNA high-expressing cells) were treated with anti-EphA10 mAb or the isotype control mAb (20 μg/ml), and then with Alexa Flour 488 conjugated anti-mouse IgG antibody. EphA10 protein expression was detected by confocal microscopy. Blue and green signals relate to DAPI and EphA10, respectively. (C) EphA10 mRNA expression levels in clinical prostate cancer tissues (39 cases) and the normal prostate tissues (9 cases) were quantified in the same method with (A). N.D. means not detectable. (D) TMAs with clinical prostate cancer tissues (39 cases) and the normal tissues (10 cases) were stained using anti-EphA10 mAb. Representative images of normal breast tissue (positive ratio: 0%), EphA10 negative cancer tissue, and EphA10 positive cancer tissues (positive ratio: 36%) are shown. Scale bar: 200 μm.

was scored as 0 (0%), 1 (1–50%), and 2 (51–100%). In terms of quantity, the signal intensity was scored as 0 (no signal), 1 (weak), 2 (moderate) or 3 (marked). Cases with a total score of more than 3 were classified into the high expression group.

2.5. Complement-dependent cytotoxicity (CDC) assay

VCaP cells were seeded at 2×10^4 cells/well in a 96 well cell culture plate (Thermo Fisher Scientific Inc., Waltham, MA) and cultured overnight. After removing the medium, antibodies (anti-EphA10 antibody or the isotype control antibody) and mouse serum as complement were added and incubated for 24 h. Cytotoxicity was evaluated using the WST-8 assay.

3. Results and discussion

3.1. EphA10 mRNA was overexpressed not only in breast cancer cell lines but also in prostate and colon cancer cell lines

In order to screen the types of cancer in which EphA10 is expressed, EphA10 mRNA expression was analyzed not only in breast cancer cells in which we had already shown EphA10

expression, but also in cell lines of colon cancer, gastric cancer, leukemia, lung cancer, melanoma, mesothelioma, pancreas cancer, prostate cancer and testicular germ cell tumors by real time PCR. EphA10 mRNA was expressed by normalizing the actin-beta expression level and represented as the ratio against normal human mammary epithelial primary cells (HMEC). Quantitative analysis demonstrated that EphA10 was expressed not only in breast cancer cells (HCC1599: 103x, MDA-MB468: 141x, DU4475: 181x), but also in prostate cancer cells (22Rv1: 142x, LNCaP: 194x) and colon cancer cells (HCT116: 107x) by more than 100 fold over human mammary epithelial primary cells (HMECs). EphA10 mRNA expression level in breast cancer cell lines was equivalent to that in prostate cancer cell lines (Fig. 1). These data suggested that EphA10 could also be associated with prostate cancers. Therefore, we next focused on prostate cancers and analyzed in more detail the expression of EphA10 at the mRNA and protein levels in cancer cell lines and clinical tissues.

3.2. EphA10 was overexpressed in prostate cancer cell lines and clinical prostate tumor tissues at mRNA and protein level

In order to examine EphA10 expression in prostate cancers, EphA10 expression at the mRNA and protein levels was evaluated in five prostate cancer cell lines (22Rv1, DU145, LNCaP, PC3 and VCaP) and normal human prostate epithelial primary cells (PrECs). Fig. 2(A) shows EphA10 was highly expressed in all cancer cell lines compared to the normal cells. Furthermore, we also analyzed EphA10 expression at the protein level in these cells. Immunofluorescent staining showed that EphA10 expression could not be detected in both PrEC and PC3 (EphA10 mRNA low-expressing cells). On the other hand, EphA10 protein expression was only observed in anti-EphA10 antibody-treated VCaP cells (EphA10 mRNA high-expressing cells), but not in the isotype control antibody-treated VCaP cells (Fig. 2(B)). These data are consistent with the pattern of EphA10 mRNA expression, further demonstrating that EphA10 was overexpressed in prostate cancer cell lines compared to the normal cells.

In order to pursue the overexpression of EphA10 in prostate cancers, we next analyzed EphA10 expression in clinical prostate cancer tissues and in normal prostate tissues. EphA10 expression at the mRNA level was first evaluated using cDNA derived from clinical prostate tumor tissues and the normal prostate tissues. A real time PCR analysis showed that EphA10 mRNA could not be amplified in all 9 normal prostate cases and 27 prostate tumor cases. In contrast, EphA10 expression was observed in 12 prostate tumor cases (approximately 31% in total cases) (Fig. 2(C)). Furthermore, we analyzed the EphA10 protein expression by IHC-staining TMA with clinical prostate cancer tissues and the normal tissues. TMA data showed that EphA10 expression was observed in 14 prostate cancer cases (approximately 36% in total cases), but not in 10 normal prostate tissues and in 25 prostate cancer cases. These data suggested that EphA10 was definitely overexpressed in prostate cancer cell lines as well as in clinical prostate tumor tissues.

We previously showed that EphA10 expression was positively associated with stage progression and lymph node metastasis in clinical breast cancers [18]. Thus, in order to evaluate the role of EphA10 overexpression in prostate cancers, we tried to analyze the relationship between EphA10 expression in clinical prostate cancer tissues and the clinical information such as the size and spread of primary tumor (pT), regional lymph node metastasis (pN), the distant metastasis (pM), and the cancer progression (pStage). Statistical analysis showed that EphA10 expression was not significantly associated with all of the above factors (Supplementary Table S1). It was reported that some Eph receptor members were overexpressed in various kinds of cancers such as breast and prostate [2], and activated by hetero-dimerizing between Eph receptors [19,20]. Therefore, in addition to focusing only on EphA10, analysis of other Eph receptors are needed in order to reveal the role of EphA10 in prostate cancers.

3.3. Anti-EphA10 mAb significantly caused complement-dependent cytotoxicity (CDC) activity dependent on EphA10 expression

In order to evaluate the potential of EphA10 as a target for prostate cancer therapy, we analyzed CDC effects of anti-EphA10 mAb on VCaP cells in which EphA10 was highly expressed. We added anti-EphA10 mAb and mouse serum as complements into VCaP cells and evaluated cytotoxicity on the next day. Fig. 3 shows that cytotoxicity in VCaP was observed only in the co-culture group of anti-EphA10 mAb and mouse serum, but not in the co-culture group of isotype control mAb and mouse serum as well as in mAb alone group. The data indicated that the cytotoxicity of anti-EphA10 mAb was dependent on EphA10 expression, and suggested that EphA10 targeted therapy might be effective in EphA10 positive prostate cancer cases.

Since molecular targeted drugs such as antibody drugs show therapeutic effects related to affinity and specificity for each antigen, it is important that the target protein display enriched expression in cancer tissues. In this respect, we previously reported that EphA10 expression was not observed in almost all normal human organs, except for testis [16]. In order to develop anti-EphA10 mAb therapy and apply it to male patients, EphA10 function in the testis should be analyzed and consider the effects of anti-EphA10 mAb on dysfunction of the testis. On the other hand, many prostate cancer patients are surgically or medically castrated with the purpose of reducing the amount of androgens which promote the growth of prostate cancer cells. However, almost all of the patients have a recurrence which is known as castration-resistant prostate cancer (CRPC). CRPCs are a bottleneck for prostate cancer therapy, because CRPCs have no effective treatment and poor prognosis. Clinical trials of antibody drugs (such as anti-CTLA4 mAb or anti-PD1 mAb) against CRPCs are currently in progress. However the therapeutic effects have been insufficient [21], emphasizing that a novel drug target is urgently needed. In this respect, EphA10 might be a promising target at least for CRPC patients, although further basic experiments are needed such as EphA10 expression analysis in CRPC cases.

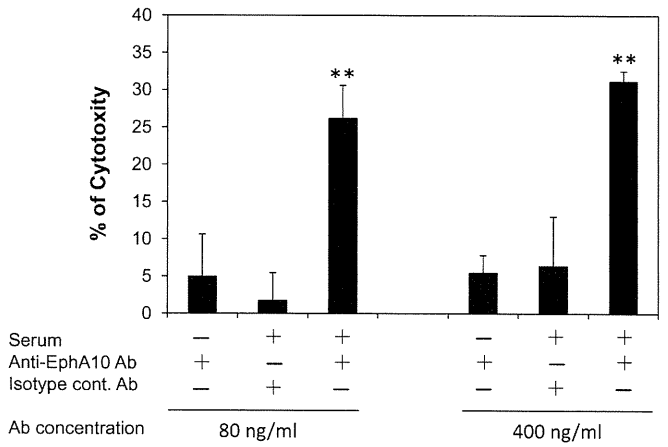

Fig. 3. Complement-dependent cytotoxicity (CDC) effects of anti-EphA10 mAb on VCaP cells. Anti-EphA10 mAb or the isotype control mAb (80 and 400 ng/ml) with/without mouse serum as complements were added to VCaP cells. After 24 h incubation, CDC effects were assessed by WST-8 assay. $^{**}p < 0.01$ vs the isotype control mAb with mouse serum. $n = 3$ in each group. Error bars represent the SD.

In conclusion, we showed that EphA10 was overexpressed in prostate cancers and suggest that EphA10 is a potential target for prostate cancer therapy.

Conflict of interest statement

The authors have no conflict of interest.

Acknowledgments

This study was supported in part by Grants-in-Aid for Scientific Research from the Project for Development of Innovative Research on Cancer Therapeutics, the Ministry of Education, Culture, Sports, Science and Technology of Japan, and from the Japan Society for the Promotion of Science. This study was also supported in part by Health Labor Sciences Research Grants from the Ministry of Health, Labor and Welfare of Japan.

Appendix A. Supplementary data

Supplementary data associated with this article can be found, in the online version, at http://dx.doi.org/10.1016/j.bbrc.2014.06.007.

References

[1] A.L. Nelson, E. Dhimolea, J.M. Reichert, Development trends for human monoclonal antibody therapeutics, Nat. Rev. Drug Discov. 9 (2010) 767–774.
[2] H.Q. Xi, X.S. Wu, B. Wei, L. Chen, Eph receptors and ephrins as targets for cancer therapy, J. Cell. Mol. Med. 16 (2012) 2894–2909.
[3] D.M. Brantley-Sieders, G. Zhuang, D. Hicks, W.B. Fang, Y. Hwang, J.M. Cates, K. Coffman, D. Jackson, E. Bruckheimer, R.S. Muraoka-Cook, J. Chen, The receptor tyrosine kinase EphA2 promotes mammary adenocarcinoma tumorigenesis and metastatic progression in mice by amplifying ErbB2 signaling, J. Clin. Invest. 118 (2008) 64–78.
[4] N. Munarini, R. Jager, S. Abderhalden, G. Zuercher, V. Rohrbach, S. Loercher, B. Pfanner-Meyer, A.C. Andres, A. Ziemiecki, Altered mammary epithelial development, pattern formation and involution in transgenic mice expressing the EphB4 receptor tyrosine kinase, J. Cell. Sci. 115 (2002) 25–37.
[5] S.R. Kumar, J. Singh, G. Xia, V. Krasnoperov, L. Hassanieh, E.J. Ley, J. Scehnet, N.G. Kumar, D. Hawes, M.F. Press, F.A. Weaver, P.S. Gill, Receptor tyrosine kinase EphB4 is a survival factor in breast cancer, Am. J. Pathol. 169 (2006) 279–293.
[6] K.A. Mohammed, X. Wang, E.P. Goldberg, V.B. Antony, N. Nasreen, Silencing receptor EphA2 induces apoptosis and attenuates tumor growth in malignant mesothelioma, Am. J. Cancer Res. 1 (2011) 419–431.
[7] N.K. Noren, M. Lu, A.L. Freeman, M. Koolpe, E.B. Pasquale, Interplay between EphB4 on tumor cells and vascular ephrin-B2 regulates tumor growth, Proc. Natl. Acad. Sci. U.S.A. 101 (2004) 5583–5588.
[8] S. Sawamiphak, S. Seidel, C.L. Essmann, G.A. Wilkinson, M.E. Pitulescu, T. Acker, A. Acker-Palmer, Ephrin-B2 regulates VEGFR2 function in developmental and tumour angiogenesis, Nature 465 (2010) 487–491.
[9] D.M. Brantley-Sieders, W.B. Fang, D.J. Hicks, G. Zhuang, Y. Shyr, J. Chen, Impaired tumor microenvironment in EphA2-deficient mice inhibits tumor angiogenesis and metastatic progression, FASEB J. 19 (2005) 1884–1886.
[10] X.D. Ji, G. Li, Y.X. Feng, J.S. Zhao, J.J. Li, Z.J. Sun, S. Shi, Y.Z. Deng, J.F. Xu, Y.Q. Zhu, H.P. Koeffler, X.J. Tong, D. Xie, EphB3 is overexpressed in non-small-cell lung cancer and promotes tumor metastasis by enhancing cell survival and migration, Cancer Res. 71 (2011) 1156–1166.
[11] A.W. Boyd, P.F. Bartlett, M. Lackmann, Therapeutic targeting of EPH receptors and their ligands, Nat. Rev. Drug Discov. 13 (2014) 39–62.
[12] D. Jackson, J. Gooya, S. Mao, K. Kinneer, L. Xu, M. Camara, C. Fazenbaker, R. Fleming, S. Swamynathan, D. Meyer, P.D. Senter, C. Gao, H. Wu, M. Kinch, S. Coats, P.A. Kiener, D.A. Tice, A human antibody-drug conjugate targeting EphA2 inhibits tumor growth in vivo, Cancer Res. 68 (2008) 9367–9374.
[13] J.W. Lee, R.L. Stone, S.J. Lee, E.J. Nam, J.W. Roh, A.M. Nick, H.D. Han, M.M. Shahzad, H.S. Kim, L.S. Mangala, N.B. Jennings, S. Mao, J. Gooya, D. Jackson, R.L. Coleman, A.K. Sood, EphA2 targeted chemotherapy using an antibody drug conjugate in endometrial carcinoma, Clin. Cancer Res. 16 (2010) 2562–2570.
[14] C.M. Annunziata, E.C. Kohn, P. LoRusso, N.D. Houston, R.L. Coleman, M. Buzoianu, G. Robbie, R. Lechleider, Phase 1, open-label study of MEDI-547 in patients with relapsed or refractory solid tumors, Invest. New Drugs 31 (2013) 77–84.
[15] S. Imai, K. Nagano, Y. Yoshida, T. Okamura, T. Yamashita, Y. Abe, T. Yoshikawa, Y. Yoshioka, H. Kamada, Y. Mukai, S. Nakagawa, Y. Tsutsumi, S. Tsunoda, Development of an antibody proteomics system using a phage antibody library for efficient screening of biomarker proteins, Biomaterials 32 (2011) 162–169.
[16] K. Nagano, Y. Maeda, S. Kanasaki, T. Watanabe, T. Yamashita, M. Inoue, K. Higashisaka, Y. Yoshioka, Y. Abe, Y. Mukai, H. Kamada, Y. Tsutsumi, S. Tsunoda, Ephrin receptor A10 is a promising drug target potentially useful for breast cancers including triple negative breast cancers, J. Control Release, in press.
[17] H.C. Aasheim, S. Patzke, H.S. Hjorthaug, E.F. Finne, Characterization of a novel Eph receptor tyrosine kinase, EphA10, expressed in testis, Biochim. Biophys. Acta 1723 (2005) 1–7.
[18] K. Nagano, S. Kanasaki, T. Yamashita, Y. Maeda, M. Inoue, K. Higashisaka, Y. Yoshioka, Y. Abe, Y. Mukai, H. Kamada, Y. Tsutsumi, S. Tsunoda, Expression of Eph receptor A10 is correlated with lymph node metastasis and stage progression in breast cancer patients, Cancer Med. 2 (2013) 972–977.
[19] B.P. Fox, R.P. Kandpal, A paradigm shift in EPH receptor interaction: biological relevance of EPHB6 interaction with EPHA2 and EPHB2 in breast carcinoma cell lines, Cancer Genomics Proteomics 8 (2011) 185–193.
[20] A. Freywald, N. Sharfe, C.M. Rolfman, The kinase-null EphB6 receptor undergoes transphosphorylation in a complex with EphB1, J. Biol. Chem. 277 (2002) 3823–3828.
[21] S.L. Topalian, F.S. Hodi, J.R. Brahmer, S.N. Gettinger, D.C. Smith, D.F. McDermott, J.D. Powderly, R.D. Carvajal, J.A. Sosman, M.B. Atkins, P.D. Leming, D.R. Spigel, S.J. Antonia, L. Horn, C.G. Drake, D.M. Pardoll, L. Chen, W.H. Sharfman, R.A. Anders, J.M. Taube, T.L. McMiller, H. Xu, A.J. Korman, M. Jure-Kunkel, S. Agrawal, D. McDonald, G.D. Kollia, A. Gupta, J.M. Wigginton, M. Sznol, Safety, activity, and immune correlates of anti-PD-1 antibody in cancer, N. Engl. J. Med. 366 (2012) 2443–2454.